DEUTSCHES ELEKTRONEN-SYNCHROTRON DESY

DESY 84-057
June 1984

DETERMINATION OF α_s IN FIRST AND SECOND ORDER QCD FROM e^+e^- ANNIHILATION INTO HADRONS

by

TASSO Collaboration

ISSN 0418-9833

NOTKESTRASSE 85 · 2 HAMBURG 52

To be sure that your preprints are promptly included in the
HIGH ENERGY PHYSICS INDEX ,
send them to the following address (if possible by air mail) :

DESY
Bibliothek
Notkestrasse 85
2 Hamburg 52
Germany

Determination of α_s in First and Second Order QCD from e^+e^- Annihilation into Hadrons

TASSO Collaboration

M.Althoff, W.Braunschweig, F.J.Kirschfink, K.Lübelsmeyer, H.-U.Martyn, P.Rosskamp, H.G.Sander[+], D.Schmitz, H.Siebke, W.Wallraff
I. Physikalisches Institut der RWTH Aachen, Germany[§]

J.Eisenmann, H.M.Fischer, H.Hartmann, A.Jocksch, G.Knop, L.Köpke[++], H.Kolanoski, H.Kück, V.Mertens, R.Wedemeyer,
Physikalisches Institut der Universität Bonn, Germany[§]

A.Eskreys[‡], K.Gather, H.Hultschig, P.Joos, U.Kötz, H.Kowalski, A.Ladage, B.Löhr, D.Lüke, P.Mättig, D.Notz, R.J.Nowak[‡‡], J.Pyrlik, M.Rushton, W.Schütte, D.Trines, T.Tymieniecka[‡‡], G.Wolf, G.Yekutieli[‡‡‡], Ch.Xiao[*]
Deutsches Elektronen-Synchrotron DESY, Hamburg, Germany

R.Fohrmann, E.Hilger, T.Kracht, H.L.Krasemann, P.Leu, E.Lohrmann, D.Pandoulas, G.Poelz, K.U.Pösnecker, B.H.Wiik
II. Institut für Experimentalphysik der Universität Hamburg, Germany[§]

R.Beuselinck, D.M.Binnie, P.Dornan, B.Foster, D.A.Garbutt, C.Jenkins, T.D.Jones, W.G.Jones, J.McCardle, K.J.Sedgbeer, J.Thomas, W.A.T. Wan Abdullah[**]
Department of Physics, Imperial College London, England[§§]

K.W.Bell, M.G.Bowler, P.Bull, R.J.Cashmore, P.E.L.Clarke, R.Devenish, P.Grossmann, C.M.Hawkes, S.L.Lloyd, C.Youngman
Department of Nuclear Physics, Oxford University, England[§§]

G.E.Forden, J.C.Hart, J.Harvey, D.K.Hasell, D.H.Saxon
Rutherford Appleton Laboratory, Chilton, England[§§]

F.Barreiro, S.Brandt, M.Dittmar, M.Holder, G.Kreutz, B.Neumann
Fachbereich Physik der Universität-Gesamthochschule Siegen, Germany[§]

E.Duchovni, Y.Eisenberg, U.Karshon, G.Mikenberg, R.Mir, D.Revel, E.Ronat, A.Shapira, M.Winik
Weizmann Institute, Rehovot, Israel[§§§]

G.Baranko, T.Barklow[***], A.Caldwell, M.Cherney, J.M.Izen, M.Mermikides, G.Rudolph, D.Strom, M.Takashima, H.Venkataramania, E.Wicklund, Sau Lan Wu, G.Zobernig
Department of Physics, University of Wisconsin, Madison, Wisconsin, USA[§§§§]

June 1984
submitted to Z. Phys. C.

+ Now at CERN, Geneva, Switzerland
++ Now at University of California, Santa Cruz, CA, USA
‡ On leave from Institute of Nuclear Physics, Cracow, Poland
‡‡ On leave from Warsaw University, Poland
‡‡‡ On leave from Weizmann Institute, Rehovot, Israel
* Now at University of Science and Technology of China, Hefei
** On leave from Universiti Malaya, Kuala Lumpur
*** Now at SLAC, Stanford, CA, USA

§ Supported by the Deutsches Bundesministerium für Forschung und Technologie
§§ Supported by the UK Science and Engineering Research Council
§§§ Supported by the Minerva Gesellschaft für Forschung mbH
§§§§ Supported by the US Department of Energy contract DE-AC02-76ER00881

Abstract

Multihadron events produced by e^+e^- annihilation at a c.m. energy of 34.6 GeV have been used to determine α_s. The predictions of 1st and 2nd order QCD models with independent jet and string fragmentation have been compared to a large variety of kinematic variables such as event shapes, transverse momentum spectra, jet masses, 3-cluster thrust and the asymmetry of energy-energy correlations. The value of α_s has been found to depend on the variables used, on the fragmentation model and on the treatment of soft gluons in the 2nd order QCD calculation. Within the models considered α_s has been found in complete 2nd order QCD to lie between 0.12 and 0.23.

1. Introduction

The three-jet events observed [1] in e^+e^- annihilation into hadrons at high c.m. energy (W ≈ 30 GeV) have given direct evidence for gluon bremsstrahlung as predicted by QCD [2]. Since the rate of three-jet events is directly proportional to the strong coupling constant α_s, a measurement of the three-jet cross section should permit a reliable measurement of α_s. However, the extraction of α_s from the data is complicated by the fact that the QCD prediction is made at the parton level. For comparison with the data one has to combine the QCD calculation with a model that describes in a phenomenological way the fragmentation of quarks and gluons into hadrons.

In an earlier publication [3] we have reported a measurement of α_s using the models of Refs. 4, 5 where quarks and gluons fragment independently and where Field-Feynman [6] fragmentation functions are employed. In this model the value of α_s has been found to be insensitive to variations of the fragmentation parameters within a broad range. Subsequently, the CELLO group [7,8] has observed that a considerably larger α_s is obtained if instead the Lund scheme [9] is used where fragmentation proceeds along the color strings between quarks and gluons. However, no or only little fragmentation scheme dependence has been found by the JADE [10] and MARK J [11] collaborations.

Besides fragmentation another potential source of uncertainty in the determination of α_s are the higher order corrections to the single gluon bremsstrahlung process. In our previous determination of α_s the second order diagrams leading to 4-parton final states [12] were included in addition to the first order diagrams. Subsequently, several theoretical groups [13-15] have computed the complete second order corrections which include the loop diagrams of the 3-parton final states. Using these calculations significantly smaller α_s values compared to the first order results have been obtained by the JADE [10], MARK J [11] and CELLO [8] collaborations.

In the present analysis we compared our data from e^+e^- annihilation into hadrons at an average c.m. energy of 34.6 GeV with QCD plus

fragmentation models and extracted α_s. A large variety of kinematic quantities was considered. The independent jet as well as the color string scheme were used to describe fragmentation. For the $O(\alpha_s^2)$ corrections to the 3-jet cross-section we considered both a) the FKSS [14] calculation to which we added the 4-parton terms with one soft or two collinear quarks (Extended FKSS) [22], and b) the AB [16] calculation based on the ERT [13] matrix elements.

2. Event Selection

The experiment was performed with the TASSO detector at PETRA. The data used for this analysis were taken at c.m. energies in the range $33 < W < 36.6$ GeV with the bulk of the data between 34 and 35 GeV. Hadronic final states from e^+e^- annihilation were selected using the information on charged particle momenta measured in the central detector. The selection criteria for charged particles and for multihadron events were identical to those described in Ref. 17. Basically, a charged track had to have a momentum component transverse to the beam of $p_{xy} > 0.1$ GeV/c and a cosine of the polar angle of $|\cos\theta| < 0.87$. The r.m.s. momentum resolution including multiple scattering was $\sigma_p/p = 0.016\ (1 + p^2)^{1/2}$, with p in GeV/c. The main criterion which the multihadron events had to satisfy was that the momentum sum of the accepted charged particles $\sum_i p_i > 0.265$ W. An additional cut was made to remove events with $\sum_i p_i/W > 2$. A total of 21315 events were accepted. To ensure a large acceptance for charged particles in jets we required $|\cos\theta_j| < 0.7$ where θ_j is the angle of the jet axis of the event and the beam direction. The number of events satisfying this cut was 16882 or 16219 depending on whether the $T^{(1)}$ or the $T^{(2)}$ momentum tensor (to be defined in Sect. 5.1) was used for the axis determination. We corrected our experimental distributions for the effect of acceptance and for QED radiative effects. This will be described in more detail in Sect. 5.

3. QCD calculation to second order in α_s

QCD predictions to second order in α_s for jet production in e^+e^- annihilation were presented for the first time by Ali et al. [12]. These included only the diagrams leading to $q\bar{q}gg$ and $q\bar{q}q\bar{q}$ final states. Complete (apart from the virtual corrections to $e^+e^- \to q\bar{q}$) second order calculations including the loop corrections to $e^+e^- \to q\bar{q}g$ were carried out by ERT [13], FKSS [14] and VGO [15], with conflicting results. In the case of ERT and VGO the $O(\alpha_s^2)$ corrections were large whereas FKSS found them to be small. The main reasons for the discrepancy are the use of different definitions for when 2 partons i and j are called 2 separate jets, the use of different variables [18, 19] and a different treatment of soft gluons. FKSS [14] used a jet definition of the Sterman-Weinberg type: 2 partons are counted as 2 separate jets if both energies are larger than $\varepsilon W/2$ and the angle between them is larger than δ. According to the experimental results on jets a reasonable set of ε, δ values is 0.2, 40° which corresponds to a scaled invariant mass squared $y = M_{ij}^2/W^2$ of about 0.01 - 0.03. In contrast, VGO considered i and j as 2 separate jets if $y > 10^{-5}$ corresponding to $M_{ij} > 0.1$ GeV at W = 35 GeV. This is an extremely small cut-off compared to the mass of an experimentally observed quark jet which is typically several GeV.

As has been pointed out in Refs. 19, 20, the ERT and VGO calculations used "bare" parton variables like thrust which are uniquely defined, whereas FKSS expressed their results in terms of "dressed" jet variables. However, in the limit of $\varepsilon, \delta \to 0$ (or $y \to 0$) the discrepancy vanishes: the sum of all $O(\alpha_s^2)$ terms as computed by FKSS approaches the corresponding result of ERT and VGO [20]. The approach occurs from below. At nonzero values of the resolution parameters, the $O(\alpha_s^2)$ calculation of the 3-jet cross-section as formulated in terms of "dressed" jet energies has problems:

> Different ways of computing 3 "dressed" jet energies from 4 partons are conceivable. If 2 partons are collinear within δ, either their energies or their 3-momenta can be added to give the energy of a single mass-less parton. The difference between the results obtained with these two schemes was found to be negligible [21]. A soft large angle gluon which is not accepted as a separate jet because of its small energy can be treated in either one of the following ways: a) it can be combined with another parton either randomly or such that the invariant mass is minimized (minimum mass recombination); b) it can be omitted from the event; to restore the total energy in this case the remaining 3 parton energies are rescaled. The latter is the scheme of Sterman-Weinberg and was adopted by FKSS. Based on a study [22] of the dressed thrust distribution it was estimated that for e.g. $\alpha_s = 0.15$ and $\varepsilon, \delta = 0.2, 40°$, α_s decreases by about 15% if, instead of the Sterman-Weinberg scheme, the minimum mass recombination scheme is employed.

Furthermore, terms of order ε and δ^2 (or y) have been neglected in the FKSS calculation. A study [22] of the dressed thrust distribution showed that for e.g. $\alpha_s = 0.15$ and $\varepsilon, \delta = 0.2, 40°$, α_s decreases by about 11% if all the missing terms were included. Of the 11%, 5% arise from approximations in the analytic calculation of FKSS, 6% arise from $q\bar{q}gg$ and $q\bar{q}q\bar{q}$ states where either one quark is soft and at large angle or two quarks are collinear within the resolution criterion. These states were inserted into the event generator used for the present analysis (Extended FKSS). Note, the $g \to q\bar{q}$ divergency which arises when $q\bar{q}$ are collinear is already contained in FKSS.

For the present analysis the Extended FKSS scheme was chosen; the α_s values were not corrected for the estimated 5% error mentioned above. The 3-jet cross section as given by the sum of the first order and the second order FKSS expressions was used to generate 3 partons which were treated as $q\bar{q}g$ in fragmentation. The hard and noncollinear 4-parton events ($q\bar{q}gg$ and $q\bar{q}q\bar{q}$) were generated according to Ali et al. [12]. The extension of FKSS consists of 3-jet-like 4-parton configurations where either one quark is soft and at large angle or 2 quarks are collinear. As far as fragmentation is concerned these states were treated as 4-parton states. The separation between 2-, 3- and 4-jet events is achieved with energy-angle (ε, δ) cuts.

In the case of energy-energy correlations the analysis was also made with the second order corrections to the 3-jet cross section as calculated by AB [16]. This calculation involves the numerical integration of the ERT matrix elements. The use of Monte Carlo techniques allowed us to impose (ε, δ) cuts or any other resolution criterion by redefining the available phase space. In contrast to the Sterman-Weinberg procedure used by FKSS, soft large angle partons which are not accepted as separate jets are recombined with that parton with which the smallest invariant mass is formed (minimum mass recombination). The resulting equivalent three-parton state was assigned to the three jet category if the corresponding ε, δ cuts were satisfied; else it was assigned to the 2-jet category.

4. Fragmentation Models

Starting from the identical QCD generator, two different fragmentation schemes were considered to fragment the partons into hadron jets.

4.1 Independent jet model [4,5]

In the Independent jet model (IJ) the partons are assumed to fragment independently from each other apart from the overall energy-momentum and flavor conservation imposed at the end of the fragmentation process. The fragmentation of quarks follows the Field-Feynman scheme [6]:

4.1.1 The primordial fragmentation function $f^h(z)$ of a quark into a hadron, $q \to q' + h$, is expressed in terms of the scaling variable $z = (E + p_L)_h/(E + p)_q$ where p_L is the momentum component of the hadron h along the quark direction. For light quarks (u, d, s) we used the form [9]

$$f^h(z) \propto (1 - z)^{a_L}, \quad a_L > 0. \qquad (1)$$

This differs from the original proposal by Field and Feynman,

$f^h(z) = 1 - a_F + 3a_F(1 - z)^2$. We found that equ. (1) gives a better description of the charged particle momentum spectrum. For the heavy quarks (c, b) the fragmentation function suggested by Peterson et al. [23] was used

$$f^h(z) \propto \frac{1}{z(1 - \frac{1}{z} - \frac{\varepsilon}{1 - z})^2} \qquad (2)$$

We used $\varepsilon_c = 0.18$ for c quarks [24] and $\varepsilon_b = 0.04$ for b quarks [25]. The precise value of ε is not important for the α_s determination.

4.1.2 The distribution of the squared transverse momentum q_T^2 of the quark q' was assumed to be of the form

$$d\sigma/dq_T^2 \propto \exp(-q_T^2/2\sigma_q^2) \qquad (3)$$

with a flavor independent parameter σ_q. The assumption of flavor independence of σ_q is supported by our recent measurement [26] of the transverse momentum distribution of charmed D* mesons.

4.1.3 For the fragmentation into mesons only pseudoscalar (P) and vector (V) meson production was considered. The production ratio P/(P+V) in the primordial cascade was set to 0.42 as determined by us from ρ° production [27] analyzed with the Hoyer et al. [4] Monte Carlo program. We fixed this ratio despite its large error [0.42 ± 0.08 (stat.) ± 0.15 (syst.)] since it is strongly correlated with the parameter a_L.

4.1.4 The production ratio of strange to nonstrange $q\bar{q}$ pairs from the vacuum was set to

$$\frac{P(s)}{P(u)} = \frac{P(s)}{P(d)} = 0.4. \qquad (4)$$

In this way reasonable agreement was obtained with our measured average of the K° and K^+ cross sections [28, 29].

4.1.5 Fragmentation into baryons was described with the model by Meyer [30]. Baryons are produced by assuming that besides $q\bar{q}$ pairs also diquark-antidiquark pairs (qq, $\bar{q}\bar{q}$) are picked up from the sea with a relative probability set to

$$\frac{P(qq)}{P(q)} = 0.11. \qquad (5)$$

Only the lowest lying octet (O) and decuplet (D) baryons are formed with the ratio O/D set equal to P/V. In this way a reasonable description of our measured p, Λ and Ξ yields was obtained [28,31,32].

4.1.6. For the fragmentation of gluons two possibilities were considered :

- The simplest assumption is that a gluon fragments like a light quark [4]. This is realized in the model by assuming that the gluon converts into a $q\bar{q}$ pair of the u, d, or s type and imparts all its momentum to one of the quarks.

- The gluon converts into a $q\bar{q}$ pair such that the gluon momentum is shared by the q and $\bar{q}$ in the proportion given by the Altarelli-Parisi splitting function [33]

$$f(z) = z^2 + (1 - z)^2, \quad z = E_q/E_g. \qquad (6)$$

The q and $\bar{q}$ which are given zero relative transverse momenta are assumed to fragment independently.

4.1.7. Experimental information [34] was used to simulate charmed particle decays. For the decays of b-flavored mesons the jet model of Ref. 35 was employed which includes weak decay matrix elements. The charged multiplicity generated by this model was found to agree with a recent measurement by the CLEO collaboration [36].

4.1.8. Energy, momentum and quantum number conservation:
The fragmentation is treated as a successive repetition of the basic process $q \rightarrow q' + h$ which is terminated when the remaining $E + p_L$ falls below a cutoff leaving unpaired a quark or a diquark in each jet. For a $q\bar{q}$ 2-jet system the quantum numbers of the last hadron generated in one of the jets are changed to ensure overall quantum number conservation. The gluon is treated analogously since it is described as a $q\bar{q}$ system.

Energy-momentum conservation is achieved in our analysis by Lorentz boosting the event into the rest system of the produced hadrons and rescaling all momenta such that the total energy is conserved. This is the procedure used in the Monte Carlo model of Ref. 5. It has recently been pointed out [8, 37] that imposing energy-momentum conservation a posteriori as done here changes the kinematic structure of $q\bar{q}g$ events and affects the determination of α_s. We shall study below the effect on α_s if energy-momentum conservation is not imposed.

4.2 The string model.

The second model considered for fragmentation was the string model developed by the Lund group [9]. In this model the colored partons are connected by color field lines (strings) which break up to form hadrons. The main difference to the IJ model shows up in the fragmentation of events containing one or more gluons. In the case of $e^+e^- \rightarrow q\bar{q}g$ the gluon corresponds to a kink in the string stretched between q and $\bar{q}$. The string breaks up near the gluon corner to form a $q_1\bar{q}_1$ pair on one side and a $q_2\bar{q}_2$ pair on the other side from which a leading hadron composed of $q_1\bar{q}_2$ is formed. The two left-over string pieces ($q\bar{q}_1$) and ($q_2\bar{q}$) fragment into hadrons in their own rest frames. Due to the string forces the hadronic final state is systematically distorted towards a more 2-jet like configuration. Consequently, to describe a given number of observed 3-jet events, the string model requires a larger value of α_s compared to the IJ model.

An ambiguity occurs in the case of 4-parton events. For instance for an $e^+e^- \to q\bar{q}g_1g_2$ event the string may be stretched in two ways from the q via the two gluons to the $\bar{q}$. We verified that either choice does not affect the value of α_s. We chose the configuration which has the smaller sum of the parton-parton mass squared, $M^2(qg_1) + M^2(\bar{q}g_2)$.

In the string model the fragmentation function of light quarks is similar to equ.(1), namely $f^h(z) \propto (1 - z)^\beta$. However, the exponent $\beta = a_L Y(m_q)$ depends on the mass of the fragmenting quark such that $Y(m_u) = Y(m_d) = 1$ and $Y(m_s) = 0.85$. Eq.(2) was used for c and b quark fragmentation. The transverse momentum distribution, the P/(P+V) and P(s)/P(u) ratios were treated in the same way as in the independent jet model and the same constants were employed for these two quantities.

For baryon production a diquark to quark rate of 0.11 was used and the parameter

$$d = \frac{P(us)\ P(d)}{P(ud)\ P(s)}$$

which acts as an extra suppression of s-quarks in diquark pairs was set equal to 0.3 leading to a good description of our p, Λ and Ξ data [28, 31, 32].

Note that in the string model, energy-momentum and the charge, flavor and baryon quantum numbers of the event are automatically conserved.

4.3 Variable fragmentation parameters.

The fragmentation parameters to be determined in the α_s fits are, for both fragmentation schemes, a_L and σ_q which control the longitudinal and transverse momentum distributions of the hadrons.

5. Event Shape and Transverse Momentum Distributions for the Determination of α_s.

The strong coupling α_s can be determined, in principle, from the rate of 3-jet (and 4-jet) events relative to that of the dominant 2-jet events. The 3-jet events produced by gluon bremsstrahlung are planar. They are therefore characterized by hadrons with large p_T in the event plane (p_T is measured relative to the jet axis of the event). On the other hand, fluctuations of the fragmentation process and the decays of heavy hadrons in genuine $e^+e^- \to q\bar{q}$ events occasionally also contribute to large p_T hadrons and therefore can lead to a correlation between α_s and the fragmentation parameters. However, the large p_T hadrons from $q\bar{q}$ events are not restricted to lie in the event plane (except in the case of hard initial state photon radiation) and therefore a simultaneous analysis of the p_T behavior in and out of the event plane allows to separate fragmentation effects from those of gluon bremsstrahlung. The correlations are taken into account by optimizing simultaneously α_s and the fragmentation parameters σ_q and a_L. For this purpose the total event sample is used. As a check, we also determined α_s by a fit to the tails of the event shape and p_T distributions which are dominated by hard gluon emission. We refer to this as the perturbative region. In this procedure we kept the fragmentation parameters fixed.

We used the following event shape measures as computed from the charged particles:

5.1 The momentum tensor.

The generalized momentum tensor is defined as

$$T^{(Y)}_{\alpha\beta} = \sum_j^N \frac{p_{j\alpha}\, p_{j\beta}}{|p_j|^{2-Y}} \Big/ \sum_j^N |p_j|^Y \qquad (7)$$

where α, β refer to the x, y, z momentum components of the j^{th} particle and N is the number of particles in an event.

We shall consider the tensors $T^{(1)}$ and $T^{(2)}$.

The tensor $T^{(2)}$ corresponds to the normalized momentum tensor introduced in Ref. 38. Diagonalization yields the unit eigenvectors $\hat{n}_1$, $\hat{n}_2$, $\hat{n}_3$ and the corresponding eigenvalues

$$Q_K = \sum_j (\vec{p}_j \cdot \hat{n}_K)^2 / \sum_j |p_j|^2 = \sum_j |p_j|^2 \cos^2\theta_{jK} / \sum_j |p_j|^2 \qquad (8)$$

Here, θ_{jK} is the angle between particle j and eigenvector k. Eq.(8) shows that $\cos^2\theta_{jk}$ is weighted by the square of the particle momentum. The Q_K satisfy the relation $Q_1 + Q_2 + Q_3 = 1$. If they are ordered such that $Q_1 < Q_2 < Q_3$ they measure the flatness (Q_1), the width (Q_2) and the length (Q_3) of an event. The plane spanned by $\hat{n}_2$ and $\hat{n}_3$ is called the event plane and $\hat{n}_3$ the jet axis. The Q_K can also be expressed in terms of the transverse momentum components <u>out</u> of and <u>in</u> the event plane, $p_{T\ out\ j}^{(Q)} = |\vec{p}_j \cdot \hat{n}_1|$, $p_{T\ in\ j}^{(Q)} = |\vec{p}_j \cdot \hat{n}_2|$:

$$Q_1 = \langle p_{T\ out}^2 \rangle / \langle p^2 \rangle \qquad (9)$$
$$Q_2 = \langle p_{T\ in}^2 \rangle / \langle p^2 \rangle$$

where the averages are taken over the particles of an event. The sphericity (S) and aplanarity (A) are given by

$$S = 3/2\ (Q_1 + Q_2) = 3/2\ (1 - Q_3) \qquad (10)$$
$$A = 3/2\ Q_1$$

The use of the tensor $T^{(1)}$ has been advocated in Refs. 13, 39. Diagonalization of $T^{(1)}$ yields the eigenvectors $\hat{m}_1$, $\hat{m}_2$, $\hat{m}_3$ and corresponding eigenvalues

$$L_K = \sum_j \frac{(\vec{p}_j \cdot \hat{m}_K)^2}{|p_j|} / \sum_j |p_j| = \sum_j |p_j| \cos^2\theta_{jK} / \sum_j |p_j| \qquad (11)$$

Thus, $\cos^2\theta_{jk}$ is weighted linearly by the particle momentum. The L_K are ordered such that $L_1 < L_2 < L_3$; their significance is similar to that of the Q_K.

5.2 Jet Mass

It has been stressed in Ref. [40] that the effective masses of jets are a sensitive measure of gluon emission. We employed the following procedure: each event was divided into two hemispheres by a plane perpendicular to the jet axis $\hat{n}_3$. The effective mass M of the system of charged particles found in a hemisphere is called the jet mass. The higher (lower) jet mass in an event is denoted by M_H (M_L). The variable used is the difference of the scaled jet masses squared

$$\Delta M^2 = \frac{M_H^2 - M_L^2}{W_V^2} \qquad (12)$$

where W_V is the total observed charged energy.

5.3 Sets of distributions

In order to determine α_s, σ_q and a_L we made in turn a simultaneous fit to each of the following four sets of normalised distributions :

(1) $1/\sigma_{tot}\ d\sigma/dQ_2$, $1/\sigma_{tot}\ d\sigma/dQ_1$, $1/\sigma_{tot}\ d\sigma/dx_p$

(2) $1/\sigma_{tot}\ d\sigma/dL_2$, $1/\sigma_{tot}\ d\sigma/dL_1$, $1/\sigma_{tot}\ d\sigma/dx_p$

(3) $1/\sigma_{tot}\ d\sigma/dp_{T\ in}^{(Q)}$, $1/\sigma_{tot}\ d\sigma/dp_{T\ out}^{(Q)}$, $1/\sigma_{tot}\ d\sigma/dx_p$

(4) $1/\sigma_{tot}\ d\sigma/dp_{T\ in}^{(L)}$, $1/\sigma_{tot}\ d\sigma/dp_{T\ out}^{(L)}$, $1/\sigma_{tot}\ d\sigma/dx_p$

The x_p distribution ($x_p = 2|p|/W$ is the scaled momentum of charged particles) was included in each of the 4 sets because it is most sensitive to a_L. Note that the integrals of the x_p and p_T distributions equal the mean multiplicity of charged particles. The p_T behavior out of and in the

event plane strongly restricts the parameter σ_q. The tails of the first distribution in each set are particularly sensitive to α_s.

As a side remark we note that with the high statistics data available here it was found that α_s, σ_q and a_L can also be determined using only one distribution which can be any one of the distributions listed above.

5.4 Corrections to the experimental distributions

The experimental distributions to be shown below were computed using the charged particles measured in the central detector for the accepted events as described in Sect. 2. To these distributions corrections were applied for the effects of QED radiation in the initial state [41], detector acceptance, multiple scattering, secondary interactions, resolution and reconstruction efficiency (see also Ref. [42]). Let $N^{data}_{meas}(x)$ be the number of raw data events (or charged particles) in a bin of some variable x. The corrected number of events (or charged particles) is given by

$$N^{data}_{corr}(x) = C(x) \cdot N^{data}_{meas}(x) \qquad (13)$$

The correction factors

$$C(x) = N^{MC}_{true}(x) \; / \; N^{MC}_{meas}(x)$$

were calculated by Monte Carlo techniques using 1st order QCD and Field-Feynman fragmentation [4]. The "true" Monte Carlo distribution of any variable was computed without QED radiation and without detector effects from the primary charged particles or from those produced in the decay of particles with lifetimes less than 3.10^{-10}sec. For example, the charged particles from K^0_S and Λ decays were included, irrespective of how far away from the interaction point the decay occurred, while the charged particles from K^0_L decays were not included. The coordinate systems (eigenvectors of the momentum tensors) to which the shape variables and transverse momenta refer, were computed with all charged and neutral stable particles. In order to obtain the "measured" Monte Carlo distribution of any variable, Monte Carlo events,

which now include QED radiative effects, were generated and passed through a detailed detector simulation and through the same event reconstruction and selection programs as used for real data. For the Monte Carlo events, the event shape, p_T and x_p variables were computed from the accepted charged tracks, as for the real data. It was checked that the Monte Carlo events used for calculating the correction functions describe the data reasonably well.

We stress that the correction functions were found to be independent of the specific QCD model used. They are basically determined by the geometrical acceptance and the effect of initial state QED radiation. We checked that the determination of α_s did not depend on whether 1st or 2nd order QCD was employed or which fragmentation model was used in the calculation of the correction functions.

5.5 Fit procedure

For a given model a lattice of 4 x 4 x 4 points in the α_s, σ_q, a_L space was considered. For each lattice point 4000 Monte Carlo events were generated and the "true" distributions were calculated according to our definition (Sect. 5.4). The content of each bin of each distribution listed in Sect. 5.3 was parametrized by a 2nd order polynomial in α_s, σ_q and a_L which gave a good description of the Monte Carlo data. The best values for α_s, σ_q and a_L were obtained by a combined fit of these parameterizations to the corrected data using the computer code MINUIT [43].

6. Results of the Shape Analysis

The fits were performed in 1st and 2nd order QCD and for both, the independent and string fragmentation models, considering for each of the 4 possible cases the 4 combinations of distributions given in Sect. 5.3.

The QCD cut-off parameters ε, δ were set to the values 0.2, 40°. For the IJ model the gluon was assumed to fragment like a light quark and the values of the σ_q and a_L parameters of the gluon jet were assumed to be the

same as those of a quark jet. Energy-momentum conservation was imposed by the Lorentz boost method. The sensitivity of α_s to all of these assumptions is discussed in Sects. 6.3, 6.4 and 6.5 respectively.

The results of the fits are given in Table 1 and Figs. 1a)-k) for 1st order QCD and in Table 2 and Figs. 2a)-k) for 2nd order QCD. Considering the fact that many ad hoc assumptions enter the fragmentation models and that only 3 parameters were allowed to vary, the general agreement between the data and the models is impressive. However, formally the χ^2/d.f. is not good. The fits were carried out considering only the statistical errors which for most of the bins are at the percent level. We are therefore in a regime where either the systematic errors or failures of the models dominate the value of χ^2/d.f. For the x_p distribution we estimated the systematic uncertainties [44]. They amount to 5% for $x_p < 0.05$, 4% for $0.05 < x_p < 0.5$ and 11% for $0.5 < x_p < 0.8$. If these errors are added quadratically to the statistical errors, the χ^2/d.f. of the x_p distribution is typically reduced from 4.8 to 1.8 for independent fragmentation and from 4.2 to 1.2 for string fragmentation.

The events which enter the fits shown in Tables 1, 2 are dominantly two-jet events. We also fitted α_s using only those kinematic regions of the Q_2, L_2, $p_{T\ in}$ and ΔM^2 variables where hard gluon bremsstrahlung dominates (perturbative region). About 20% of the accepted events (6% of the accepted tracks in the case of $p_{T\ in}$) fall into these regions as defined in Tables 3,4. The parameters σ_q and a_L were fixed at their average values obtained from the 4 sets of distributions shown in Tables 1, 2. The resulting α_s values are given in Tables 3,4.

6.1 Discussion of the first order QCD fits.

Within each model, the 4 sets of distributions give consistent results for the fragmentation parameters. The values of σ_q and a_L are somewhat smaller in the string model than in the IJ model.

The fitted values of α_s using the IJ model range from 0.19 to 0.215 depending on the set of distributions. The string model yields a factor

1.3 - 1.5 times higher α_s values; they are in the range 0.25 to 0.29. The values of α_s as obtained from the perturbative regions agree with those from the overall fits within statistical errors.

An interesting observation [45] is that the string model predicts too few events in the tails of the Q_1, L_1 and $p_{T\ out}$ distributions, see Fig. 1. Such a discrepancy is not observed for the IJ model in contrast to Ref. 45. It is suggestive to attribute it to the fact that fragmentation of $e^+e^- \to q\bar{q}g$ events in the string picture occurs in two Lorentz frames which are different from the overall c.m. system. As a result, the events are more planar than in the IJ model. This discrepancy between the string model and the data is strongly reduced if $O(\alpha_s^2)$ terms (4-jet events) are included as will be shown below.

6.2 Discussion of the 2nd order QCD fits.

The values of the fragmentation parameters changed only little as compared to the first order fits. Their values averaged over the 4 sets of distributions are for the IJ model

$$\sigma_q = 0.35 \pm 0.01 \text{ GeV/c}$$
$$a_L = 0.61 \pm 0.06$$

and for the string model

$$\sigma_q = 0.32 \pm 0.01 \text{ GeV/c}$$
$$a_L = 0.41 \pm 0.06$$

However, the values of σ_q and a_L depend on the input value of P/(P + V). In order to estimate this dependence, two fits were performed for the IJ model where P/(P + V) was set to a) 0.25 and b) 0.60. These values mark the limits allowed by the measurement of P/(P + V) of Ref. 27.

The results are

for $P/(P + V) = 0.25$: $\sigma_q = 0.37$ GeV/c, $a_L = 0.45$

for $P/(P + V) = 0.60$: $\sigma_q = 0.32$ GeV/c, $a_L = 0.82$.

Although σ_q and a_L are strongly correlated with $P/(P + V)$, the value of α_s changed by less than 0.004.

The fitted values for α_s in the IJ model lie between 0.15 and 0.16 and are about 20% smaller than in 1st order. For the string model, the α_s values range from 0.19 to 0.22 and are about 25% lower than in 1st order. Hence, the model dependence of α_s persists also in 2nd order: the string model yields α_s values which are a factor 1.25 to 1.50 times higher than with independent fragmentation. Again, the α_s values from the perturbative regions shown in the 2nd column of Tables 3 and 4, agree with those from the total event sample within statistical errors. In particular, the α_s dependence on the fragmentation model is the same as for the overall fits.

A comparison of the fits in 1st and 2nd order QCD shows that for the IJ model the overall χ^2/d.f. values do not improve in going from 1st to 2nd order, while for the string model the fit quality shows a marked improvement when the 2nd order contribution is included. This is particularly true for the Q_1, L_1 and $p_{T\ out}$ distributions. However, in the string model the 1st and 2nd order contributions are not sufficient to completely explain the tails of these distributions.

It is observed that the x_p distribution and the $p_{T\ in}$ distribution at large values of $p_{T\ in}$ are slightly better reproduced with the string model. On the other hand, the quantities related to $p_{T\ out}$ are better described by the IJ model. As a consequence, the χ^2/d.f. values of the overall fits do not allow us to prefer one of the two fragmentation models.

6.3 Variation of ε, δ.

The Sterman-Weinberg formalism is one way to avoid divergencies in the QCD cross sections. The values of the parameters ε, δ are in principle

arbitrary. However, in order to prevent the next higher order contributions from becoming important the ε, δ parameters cannot be arbitrarily small [20]. In going from the parton to the hadron level, fragmentation has to be included. This suggests one should choose ε, δ corresponding to the typical jet spread.

We explored the dependence of α_s on the ε, δ parameters for the values (0.15, 34.5°), (0.20, 40°) and (0.25, 45°). Here, ε is chosen to be proportional to $1-\cos\delta$ [20]. Note that within this range of ε, δ values the 4-parton cross section changes by a factor of 5 (e.g. from 10% to 2% of σ_{tot} for $\alpha_s = 0.17$). The fits (not shown) for the fragmentation parameters and α_s were repeated for the lower and higher ε, δ sets. We found that the values of α_s and of the fragmentation parameters depend slightly on the choice of ε, δ. We note that the lower ε, δ values give a poorer fit than the higher ones. Tables 3 and 4 show the results of the α_s fits to the perturbative regions where a_L and σ_q were fixed to the values obtained in the overall fits for the particular choice of ε, δ. For both fragmentation models, α_s increases on average by 0.02 if ε, δ are increased within the range considered. Such a dependence is theoretically expected [20] and is a source of systematic uncertainty.

6.4 Gluon fragmentation

In contrast to the string model, the IJ model makes no prediction for gluon fragmentation. So far, we assumed that the gluon fragments into hadrons like a u, d or s quark. Experimental results from the JADE group [46] indicate that the fragmentation function of the gluon is softer and broader than that of a quark. We therefore repeated the fits using the Altarelli-Parisi proposal [33] for the gluon to split into $q\bar{q}$ before fragmenting which generates a softer hadron spectrum. The resulting α_s, σ_q and a_L parameters are given in Table 5a. The χ^2/d.f. values are systematically higher by ~2 units than obtained before (Table 2a). This may indicate that the fragmentation of two parallel quarks cannot be treated independently. The results of the α_s fits to the perturbative regions are given in Table 5b. The values of α_s obtained under the assumption of gluon

splitting are systematically higher by 0.01-0.02 and are thus closer to the values obtained with the string model.

We also tried to fit α_s under the assumption that the gluon jet is broader (σ_q = 0.5 GeV/c as suggested by Ref.46). This had a negligible effect on α_s ($\Delta\alpha_s < 0.004$).

6.5 Energy-momentum conservation.

As discussed before, the value of α_s for independent fragmentation may depend on whether or not energy-momentum is exactly conserved in the model. For the fit results presented so far, energy-momentum conservation was achieved by the Lorentz boost method (see Sect. 4.1.8). When this constraint was omitted and the event shape and p_T analysis in 2nd order QCD was repeated, no significant changes of α_s ($\Delta\alpha_s < 0.003$) and of the fragmentation parameters were observed.

6.6 Dependence on event selection cuts.

As a check on the stability of the fit results, the event selection cuts were changed and the fits were repeated. In the first fit the cut on the angle between the jet axis and the beam direction was changed ($|\cos\theta_j| < 0.8$ instead of 0.7). In the second fit a cut was placed on the angle between the normal to the event plane and the beam direction ($|\cos\theta_n| > 0.2$) which suppresses 2-jet events with a hard collinear photon radiated in the initial state. In both cases, the values of α_s and of the fragmentation parameters changed only within statistical errors.

7. Cluster Analysis for the Determination of α_s

The number of events which have 3 collimated and well separated clusters of energy allows in principle the most direct determination of α_s. Fragmentation effects are expected to play a minor role here [47]. For jet finding we used the angular algorithm described in Ref. 48. This algorithm collects particles with relative angles smaller than α into preclusters and

combines preclusters with relative angles smaller than β into clusters. The N clusters found in an event are ordered in energy $E_1 < E_2 < \ldots < E_N$. The n lowest energy clusters which satisfy the condition $\sum_{i=1}^{n} E_i < \varepsilon_1 W/2$ are removed. The remaining clusters with energies greater than $\varepsilon_2 W/2$ are called jets. The parameters (α, β, ε_1, ε_2) were chosen as (30°, 45°, 0.1, 0.145). Note that the parameters ε_1 and β of the cluster algorithm correspond to the Sterman-Weinberg ε and δ parameters used in the perturbative QCD calculation. Since our cluster analysis considered only charged particles, the value of ε_1 is half of that of ε.

For the following study events with only 3 jets were selected. The jet energies were reconstructed from the directions of the jets. For this purpose the measured jet momenta which are given by the vector sum of the particle momenta, were projected onto the event plane ($\hat{n}_2$, $\hat{n}_3$), which was determined in the event shape analysis by the $T^{(2)}$ tensor. Assuming massless jets, the angles θ_{ik} (defined as $\theta_{ik} \leq \pi$) between the projected jet momenta were used to compute the scaled reconstructed jet energies

$$x_i = 2\sin\theta_{jk}/(\sin\theta_{12} + \sin\theta_{13} + \sin\theta_{23}), \quad \text{ijk cyclic.} \qquad (14)$$

Events with momentum imbalance ($\theta_{12} + \theta_{13} + \theta_{23} < 2\pi$) were rejected. The cluster thrust is defined as $t_{CL} = \max(x_1, x_2, x_3)$. A two-jet like configuration has t_{CL} close to 1 and the configuration with all three angles equal to 120° has $t_{CL} = 2/3$.

A determination of α_s in 2nd order QCD was performed by fitting the t_{CL} distribution of the raw data to the t_{CL} distribution predicted by the Monte Carlo model. The model calculations included QED radiative effects, detector simulation and event reconstruction, and were done for the IJ model with g = q as well as for the string model. The fragmentation parameters were set to the values given in Sect. 6.2 and the ε, δ parameters were taken as 0.2, 40°.

The cluster thrust distribution of the data is shown in Fig. 3. The fits were performed in the region $t_{CL} < 0.94$ for which the $e^+e^- \to q\bar{q}$

contribution is expected to be small (<3%). The QCD models are seen to give a good description of the data for the t_{CL}-region fitted. At larger t_{CL} values more events are observed than predicted by the models. The α_s results are given in Table 6a for the cuts $t_{CL} < 0.94$, < 0.90 and < 0.85. The values of α_s depend little on the t_{CL} cut.

The values of α_s obtained in this way, viz. $\alpha_s \approx 0.14$ (0.18) for independent (string) fragmentation, are systematically lower than those obtained by the shape analysis, viz. $\alpha_s \approx 0.155$ (0.21). The ratio of $\alpha_s^{string}/\alpha_s^{IJ} = 1.29$. Thus, in contrast to the earlier hope [47] and to results from JADE [10], a significant model dependence of α_s is also observed with the cluster analysis [7]. The values of α_s were found to be stable against changes of the cluster defining parameters (α, β, ϵ_1, ϵ_2) within a broad range.

8. Determination of α_s with the Method of Generalized Sphericity

We also used the method of generalized sphericity [49] to extract 3-jet events. In distinction to the cluster method described before, this algorithm is quadratic in the particle momenta and therefore gives high momentum particles a larger weight. The particle momenta are projected onto the event plane ($\hat{n}_2$, $\hat{n}_3$) obtained from the momentum tensor $T^{(2)}$. Three nonoverlapping sets of particles are found which satisfy the requirement that the sum of the jet sphericities is a minimum. The jet directions are given by the individual jet sphericity axes.

An analysis similar to the one described in the previous section was performed to determine the 3-jet thrust t_{GS}. The distribution of t_{GS} is shown is Fig. 4 for those events in which each jet has a visible energy of more than 0.145 W/2. The distribution looks quite different from the cluster-thrust distribution. This is partly due to the fact that in the method discussed here all events are treated as 3-jet events and that each particle is assigned to one of the three jets. Consequently, the jets on average have more energy and therefore a higher chance of passing the jet energy cut. The two QCD models provide reasonable fits to the data for

$t_{GS} < 0.94$. The α_s results in 2nd order QCD from fits to the t_{GS} distribution for $t_{GS} < 0.94$, < 0.90 and < 0.85 are given in Table 6b. The values of α_s obtained with this method are very similar to those obtained from the cluster analysis; they are $\alpha_s \approx 0.14$ (0.19) for independent (string) fragmentation. Again, α_s depends on the fragmentation model : $\alpha_s^{string}/\alpha_s^{IJ} = 1.31$.

9. Determination of α_s from Energy-Energy Correlations.

Energy-energy correlations have been proposed [50, 51] to study $e^+e^- \to$ hadrons and the underlying parton structure. The energy-weighted angular correlation (EWAC) is defined as

$$\frac{1}{\sigma_{tot}} \frac{d\Sigma}{d\cos\chi} = f(\cos\chi) = \frac{1}{N} \sum_{events} \sum_{i,k} \frac{E_i \cdot E_k}{W^2} \delta(\cos\chi - \cos\chi_{ik}) \quad (15)$$

where χ_{ik} is the angle between particles i and k with energies E_i and E_k. The summation is extended over all pairs i, k of particles in an event including the case i = k, and over all N events. The normalization is therefore $\int f(\cos\chi) d\cos\chi = 1$.

The EWAC is affected by fragmentation. The fragmentation effects from $e^+e^- \to q\bar{q}$ are suppressed if instead of $f(\cos\chi)$ the asymmetry is considered:

$$A(\cos\chi) = f(\cos(\pi-\chi)) - f(\cos\chi). \quad (16)$$

In the asymmetry the contribution from hard noncollinear gluon emission relative to the $q\bar{q}$ contribution is enhanced and therefore the sensitivity to α_s is increased. However, the asymmetry still depends on the fragmentation of $e^+e^- \to q\bar{q}g$ events.

We evaluated the EWAC using only the charged particles and replacing W by the visible energy W_{vis} which is the sum of the charged particle energies in an event assuming all particles to be pions. Following Sect. 5.4, the EWAC was corrected for detector acceptance, event selection cuts and QED

initial state radiation, but not for neutral particles. From the corrected EWAC, the asymmetry A(cosχ) was obtained and is displayed in Fig. 5.

9.1 α_s in first order QCD

α_s was determined from a fit to the asymmetry in the large angle region $|\cos\chi| < 0.7$. Both fragmentation schemes were considered. The fragmentation parameters were taken from the shape analysis (Table 1). The results of the fits for the IJ model with g = q and for the string model are given in Table 7a and shown by the histograms in Fig. 5a. The value of α_s depends strongly on the fragmentation scheme as shown by the ratio $\alpha_s^{string} / \alpha_s^{IJ} = 1.52$.

9.2 α_s in second order QCD using Extended FKSS.

The same fits were repeated in 2nd order QCD using the Extended FKSS calculation and the fragmentation parameters given in Sect. 6.2. The results are given in Table 7b and shown in Fig. 5b. The agreement with the data is reasonable. The α_s values agree with the corresponding values obtained in the shape and cluster analysis. The difference between the two fragmentation schemes persists also in 2nd order: for our standard choice of parameters $\alpha_s^{string} / \alpha_s^{IJ} = 1.37$.

The value of α_s was found to be insensitive to the choice of the ε, δ parameters as shown in Table 7b. An increase of α_s of approximately 10% was found in the IJ model when, instead of g = q, the gluon was assumed to split (see Table 7b). The value of α_s dropped by a considerable amount (20%) if energy-momentum conservation was not required in the IJ model, in agreement with the observation of the CELLO group [8] and with Ref. 37. Finally, we note that increasing the $|\cos\chi|$ cut (e.g. from 0.7 to 0.8) would result in smaller α_s values.

9.3 α_s in second order QCD using AB

The fits to the asymmetry were also performed with the 2nd order calculation by AB [16]. Again, the fragmentation parameters of the IJ and

string models were taken from the shape analysis of Sect. 6.2. The α_s values are given in Table 7c. Also in this approach α_s was found to depend on the fragmentation scheme, $\alpha_s^{string} / \alpha_s^{IJ} = 1.36$ if our standard g = q assumption is used for independent fragmentation. The α_s values are 15-20% lower than the corresponding ones found with the Extended FKSS calculation. This difference is mainly attributed to the different treatment of soft partons, i.e. minimum mass recombination (AB) versus Sterman-Weinberg definition (FKSS).

10. Energy Dependence of Event Shapes.

This section compares the predictions of the 2nd order QCD models with the data at different c.m. energies.

We assumed the fragmentation parameters to be energy independent. The values given in Sect.6.2 were taken. For α_s we assumed the logarithmic W dependence as given by the 2nd order formula [52] where the QCD scale parameter Λ was fixed using the fits at W = 34.6 GeV, i.e. Λ = 0.36 GeV (1.20 GeV) for independent (string) fragmentation. At W ≦ 14 GeV only 1st order QCD was taken.

Data on event shape measures are available from this experiment covering the energy range from 12 to 43 GeV (see Ref. 42). The average values of sphericity, 1-thrust, $\langle p_{T\ in}^2 \rangle$ and $\langle p_{T\ out}^2 \rangle$ are displayed in Figs. 6a-c as a function of W. Note, in this case the sphericity and thrust distributions have been corrected such that they include also the neutral particles. The model predictions are drawn as curves. The trend of the data is reasonably well reproduced by both the independent and the string fragmentation models. The experimental observation of a slow variation of <S> and <1-T> at energies above ≈30 GeV is better reproduced in 2nd order QCD than in 1st order QCD, (compare the corresponding Figs. 21, 22 of Ref. 42).

Some deviation between the data and the model predictions occur near W = 14 GeV. This may indicate a slight energy dependence of the fragmentation parameters as expected in e.g. models of multigluon emission.

11. Discussion of the results

We have determined α_s from a data sample of 16 500 multihadron events produced by e^+e^- annihilation at an average c.m. energy of 34.6 GeV. The α_s analysis employed the 1st as well as the 2nd order QCD calculations and used both the independent jet (IJ) model and the Lund string model to describe the hadronization.

By taking into account the many measurements of identified particle spectra most of the parameters of the fragmentation models have been fixed. We have treated as the only free parameters σ_q and a_L which describe the transverse and longitudinal momentum spectra of the produced hadrons.

Using <u>all</u> events, α_s was obtained simultaneously with σ_q and a_L by fitting event shape or p_T distributions and the momentum distribution. In a second step, σ_q and a_L were fixed to the fitted values and the α_s fits were repeated considering only the perturbative regions, which are dominated by gluon bremsstrahlung. The resulting α_s values were found to be the same as those from the overall fits, within errors. The perturbative regions and the overall distributions were found to be described equally well by the QCD models. This shows that we have obtained a consistent description of the two- and three-jet regions.

All data considered, i.e. event shapes, jet masses, transverse momenta, 3-cluster thrust and the asymmetry of the energy-energy correlation, can be described by the same value of α_s to within ± 10% <u>provided</u> the same QCD calculation and the same fragmentation model is used.

The value of α_s obtained in 2nd order QCD, $(\alpha_s^{(2)})$, is always smaller than the 1st order result, $(\alpha_s^{(1)})$. The ratio $\alpha_s^{(2)}/\alpha_s^{(1)}$ depends on the QCD calculation, on the fragmentation model and on the distribution used. With the Extended FKSS scheme we have obtained:

$$\alpha_s^{(2)}/\alpha_s^{(1)} = 0.74 \text{ to } 0.84 \quad \text{for independent fragmentation and}$$

$$0.71 \text{ to } 0.76 \quad \text{for string fragmentation.}$$

With the AB scheme, a larger difference between $\alpha_s^{(2)}$ and $\alpha_s^{(1)}$ was obtained:

$$\alpha_s^{(2)}/\alpha_s^{(1)} = 0.70 \quad \text{for independent fragmentation and}$$

$$0.63 \quad \text{for string fragmentation.}$$

Thus, the way soft gluons are treated has a noticeable influence on the size of the 2nd order corrections. The 2nd order corrections are large and it is conceivable that the next higher orders are not negligible.

In the case of the string model the inclusion of the 2nd order contributions has led to a marked improvement of the fit quality for the Q_1, L_1 and $p_{T\ out}$ distributions. This is in agreement with the JADE observation [45]. In case of the IJ model, 1st and 2nd order QCD gave about the same fit quality, in contrast to Ref. 45.

The dependence of α_s on the fragmentation scheme was studied by considering two conceptually different fragmentation models, namely the independent jet and the color string models. <u>All</u> distributions used led to a fragmentation scheme dependent α_s value. In 1st order QCD the result is

$$\alpha_s^{string}/\alpha_s^{IJ,g=q} = 1.32 \text{ to } 1.60.$$

This model dependence is slightly reduced in 2nd order QCD (Extended FKSS and AB):

$$\alpha_s^{string}/\alpha_s^{IJ,g=q} = 1.22 \text{ to } 1.48$$

depending on the distribution. The smallest (largest) model dependence was seen with the $p_{T\ in}$ (ΔM^2) distribution. Our results on this model dependence are in agreement with those published by the CELLO group [7,8].

Compared to the case where gluons fragment like light quarks (g = q), the assumption of gluon splitting ($g \to q\bar{q}$) led to a smaller ratio:

$$\alpha_s^{string}/\alpha_s^{IJ,g\to q\bar{q}} = 1.08 \text{ to } 1.35.$$

However, with gluon splitting the data distributions were in general less well fitted than with the g = q assumption.

The following summarizes the α_s values obtained in 2nd order QCD for the different fragmentation models.
Using Extended FKSS:

$$\alpha_s^{IJ,g=q} = 0.14 \text{ to } 0.16$$

$$\alpha_s^{IJ,g\to q\bar{q}} = 0.16 \text{ to } 0.18$$

$$\alpha_s^{string} = 0.18 \text{ to } 0.23.$$

A comparison between the Extended FKSS and the ERT + AB schemes has been made for the case of the asymmetry of the energy-energy correlation yielding the following results:

	Extended FKSS	ERT + AB
$\alpha_s^{IJ,g=q}$	0.139	0.117
$\alpha_s^{IJ,g\to q\bar{q}}$	0.157	0.127
α_s^{string}	0.190	0.159

As mentioned in Sect. 3 the Extended FKSS calculation used for the fits involves certain approximations which affect the value of α_s. We estimate that without these approximations the α_s values given above and in Tables 1 - 7 for Extended FKSS should be reduced by about 5%.

Our results can be compared with similar determinations of α_s in full 2nd order from other experiments.

The JADE group [10] employing the unmodified FKSS calculation and assuming $g \to q\bar{q}$ in case of the IJ model, obtained from a cluster analysis $\alpha_s = 0.16 \pm 0.015 \pm 0.03$ independent of the fragmentation scheme. Within the systematic errors quoted this is consistent with our corresponding values of 0.136 ± 0.005 for the IJ model and 0.174 ± 0.007 for the string model obtained for $t_{CL} < 0.85$ (see Table 6).

The MARK-J group [11] used the ERT + AB calculation and determined α_s from the asymmetry of the energy-energy correlation. Their values, $\alpha_s = 0.12 \pm 0.01$ for the IJ, $g \to q\bar{q}$ model and $\alpha_s = 0.14 \pm 0.01$ for the string model should be compared with our values 0.127 ± 0.010 and 0.159 ± 0.012 respectively, as shown in Table 7. Our values indicate a stronger dependence on the fragmentation model.

The CELLO group [8] employed the unmodified FKSS calculation and fitted α_s to the distributions of the asymmetry and the 3-cluster thrust. Their values of $\alpha_s = 0.18 - 0.19$ for string fragmentation and $\alpha_s = 0.13 - 0.15$ for independent fragmentation (with g = q and the Lorentz boost method to conserve energy-momentum) agree with our corresponding values of 0.18 - 0.19 and 0.14, respectively, see Tables 6, 7.

In conclusion, the uncertainty in the determination of α_s is rather large. As shown above, this has several causes:

- Fits to distributions of different kinematical variables lead to α_s values which differ by up to 15 - 20 %.

- There is a complete lack of theoretical understanding of the fragmentation process. The α_s values determined with the IJ and the string model differ by about 30%. The quality of the fits to the distributions considered here has not permitted a choice between the the two models. However, the JADE group [53] from a study of other

aspects of 3-jet production, has found some preference for the string picture.

- In the independent fragmentation model energy-momentum conservation has to be put in by hand. This can be done in various ways and affects the value of α_s [8, 37]. We have used in our analysis the Lorentz boost method and have found that the difference in α_s between imposing and not imposing E - p conservation is negligible ($\Delta\alpha_s < 2\%$) for the event shape and p_T distributions while the asymmetry is strongly affected ($\Delta\alpha_s \approx 20\%$).

- Variation of the resolution parameters ε, δ within a reasonable range yielded differences in α_s of the order of 10%. The asymmetry of the energy-energy correlation is less sensitive.

- The comparison of Extended FKSS with ERT + AB has been performed for the asymmetry of the energy-energy correlation and has shown that the different treatments of soft gluons in the 2nd order QCD calculation of the 3-jet cross section leads to α_s values which differ by 10 - 15%.

Acknowledgments

We gratefully acknowledge the effort of the PETRA machine group and the support of the DESY directorate. We are grateful to Dr. P. Söding for the many useful discussions and we thank Drs. F. Gutbrod, G. Kramer, Z. Kunszt and G. Schierholz for their help on the theoretical part of this analysis. We thank the US Department of Energy and the University of Wisconsin for providing the VAX 11-780 computer on which a large part of the extensive Monte Carlo calculations for this analysis were performed. Those of us from abroad wish to thank the DESY directorate for the hospitality extended to us.

List of References.

1. TASSO Collaboration, R. Brandelik et al., Phys.Lett. 86B (1979) 243; MARK J Collaboration, D. Barber et al., Phys.Rev.Lett. 43 (1979) 830; PLUTO Collaboration, Ch. Berger et al., Phys.Lett. 86B (1979) 418; JADE Collaboration, W. Bartel et al., Phys.Lett. 91B (1980) 142.
2. J. Ellis, M.K.Gaillard, G.G.Ross, Nucl.Phys. B111 (1976) 253; T.A. DeGrand, Y.T.Ng, S.H.Tye, Phys.Rev. D16 (1977) 3251; A.DeRujula, J.Ellis, E.Floratos, M.K.Gaillard, Nucl.Phys. B138 (1978) 387: G.Kramer, G.Schierholz, J.Willrodt, Phys.Lett. 79B (1978) 249.
3. TASSO Collaboration, R.Brandelik et al.,Phys.Lett. 94B (1980) 437.
4. P.Hoyer, P.Osland, H.G.Sander, T.Walsh, P.Zerwas, Nucl.Phys. B161 (1979) 349.
5. A.Ali, E.Pietarinen, G.Kramer, J.Willrodt, Phys.Lett. 93B (1980) 155.
6. R.Field, R.Feynman, Nucl.Phys. B136 (1978) 1.
7. CELLO Collaboration, H.Behrend et al., Nucl.Phys. B218 (1983) 269.
8. CELLO Collaboration, H.J.Behrend et al., Phys.Lett. 138B (1984) 311.
9. B.Andersson, G.Gustafson, T.Sjöstrand, Phys.Lett. 94B (1980) 211; Z.Phys. C6 (1980) 235; Nucl.Phys. B197 (1982) 45; T.Sjöstrand, Computer Physics Comm. 27 (1982) 243; ibid.28 (1983) 229.
10. JADE Collaboration, W.Bartel et al., Phys.Lett. 119B (1982) 239.
11. MARK-J Collaboration, B.Adeva et al., Phys.Rev.Lett. 50 (1983) 2051.
12. A.Ali, J.Körner, Z.Kunszt, E.Pietarinen, G.Kramer, G.Schierholz, J.Willrodt, Phys.Lett. 82B (1979) 285 and Nucl.Phys. B167 (1980) 454.
13. R.K.Ellis, D.Ross, A.Terrano, Phys.Lett. 45B (1980) 1226; Nucl.Phys. B178 (1980) 421.
14. K.Fabricius, G.Kramer, G.Schierholz, I.Schmitt, Phys.Lett. 97B (1980) 431 and Z.Phys. C11 (1982) 315.
15. J.Vermaseren, J.Gaemers, S.Oldham, Nucl.Phys. B187 (1981) 301.
16. A.Ali, F.Barreiro, Phys.Lett. 118B (1982) 155; Nucl.Phys. B236 (1984) 269.
17. TASSO Collaboration, R.Brandelik et al., Phys.Lett. 113B (1982) 499.
18. A.J.Buras in Proc.Int.Symposium on Lepton and Photon Interactions at High Energies, Bonn, 1981, ed. W. Pfeil, p.636.
19. T.Gottschalk, Phys.Lett. 109B (1982) 331.

20. F.Gutbrod, G.Kramer, G.Schierholz, Z. Phys. C21 (1984) 235.
21. R.-Y.Zhu, Thesis, MIT, Nov.83.
22. F.Gutbrod, G.Rudolph, G.Schierholz, publication in preparation.
23. C.Peterson et al., Phys.Rev. D27 (1983) 105.
24. TASSO Collaboration, M. Althoff et al., Phys.Lett. 126B (1983) 493.
25. MARK II Collaboration, M.E.Nelson et al.,Phys.Rev.Lett. 50 (1983) 1542.
26. TASSO Collaboration, M.Althoff et al., Phys.Lett. 135B (1984) 243
27. TASSO Collaboration, R.Brandelik et al., Phys.Lett. 117B (1982) 135.
28. TASSO Collaboration, M.Althoff et al., Z.Phys. C17 (1983) 5.
29. TASSO Collaboration, M.Althoff et al., to be published.
30. T.Meyer, Z.Phys. C12 (1982) 77.
31. TASSO Collaboration, R.Brandelik et al., Phys.Lett. 105B (1981) 75.
32. TASSO Collaboration, M.Althoff et al., Phys.Lett. 130B (1983) 340.
33. G.Altarelli, G.Parisi, Nucl.Phys. B126 (1977) 298.
34. MARK I Collaboration, R.Schindler et al., Phys.Rev. D24 (1981) 78.
35. A.Ali, J.Körner, G.Kramer, J.Willrodt, Z.Phys. C1 (1979) 203.
36. CLEO Collaboration, M.Alam et al., Phys.Rev.Lett. 49 (1982) 357.
37. T.Sjöstrand, DESY Report 84-023.
38. J.Bjorken, S.Brodsky, Phys.Rev. D1 (1970) 1416.
39. J.Donoghue, F.Low, S.Y.Pi, Phys.Rev. D20 (1979) 2759;
G.Parisi, Phys.Lett. 74B (1978) 65.
40. L.Clavelli, H.P.Nilles, Phys.Rev. D21 (1980) 1242;
L.Clavelli, Preprint ANL-HEP-CP-83-05.
41. F.A.Berends, R.Kleiss, Nucl.Phys. B177 (1981) 237; ibid.B178 (1981) 141.
42. TASSO Collaboration, M.Althoff et al., Z.Phys. C22 (1984) 307.
43. MINUIT, CERN Program Library.
44. TASSO Collaboration, R.Brandelik et al., Phys.Lett. 114B (1982) 65.
45. JADE Collaboration, W.Bartel et al., Phys.Lett. 115B (1982) 338.
46. JADE Collaboration, W.Bartel et al., Phys.Lett. 123B (1983) 460;
Z.Phys. C21 (1983) 37.
47. G.Kramer, DESY Report 83-068 (1983), to be published in Springer
Tracts of Modern Physics.
48. H.Daum, H.Meyer, J.Börger, Z.Phys. C8 (1981) 167.
49. S.L.Wu, G.Zobernig, Z.Phys. C2 (1979) 107.
50. Y.L.Dokhshitzer, D.I.D'Yakonov, S.I.Troyan, Phys.Lett. 78B (1978) 290;
and Phys.Rep. 58 (1980) 269.
51. C.L.Basham et al., Phys.Rev.Lett. 41 (1978) 1585 and Phys.Rev. D19
(1979) 2018.
52. W. Bardeen et al., Phys.Rev. D18 (1978) 3998.
53. JADE Collaboration, W. Bartel et al., Phys.Lett. 101B (1981) 129;
Phys.Lett. 134B (1984) 275.

Table 1a: Fit results for the independent jet model, 1^{st} order QCD

Distributions (χ^2/d.f.)			overall χ^2/d.f.	α_s	σ_q (GeV/c)	a_L
$Q_2(1.2)$	$Q_1(2.9)$	x(4.7)	3.6	0.215 ± 0.005	0.354 ± 0.003	0.642 ± 0.015
$L_2(1.5)$	$L_1(3.0)$	x(5.5)	4.3	0.195 ± 0.005	0.341 ± 0.003	0.638 ± 0.015
$p_{Tin}^{(Q)}(3.7)$	$p_{Tout}^{(Q)}(3.2)$	x(5.8)	4.7	0.188 ± 0.004	0.351 ± 0.002	0.636 ± 0.011
$p_{Tin}^{(L)}(4.0)$	$p_{Tout}^{(L)}(4.3)$	x(6.2)	5.3	0.195 ± 0.004	0.344 ± 0.002	0.603 ± 0.011

Table 1b: Fit results for the Lund string model, 1^{st} order QCD.

Distributions (χ^2/d.f.)			overall χ^2/d.f.	α_s	σ_q (GeV/c)	a_L
$Q_2(2.2)$	$Q_1(9.0)$	x(3.6)	4.5	0.283 ± 0.005	0.323 ± 0.004	0.471 ± 0.018
$L_2(3.1)$	$L_1(23.0)$	x(4.1)	7.7	0.292 ± 0.005	0.319 ± 0.004	0.413 ± 0.016
$p_{Tin}^{(Q)}(3.9)$	$p_{Tout}^{(Q)}(7.9)$	x(3.8)	5.1	0.252 ± 0.004	0.336 ± 0.002	0.508 ± 0.012
$p_{Tin}^{(L)}(5.9)$	$p_{Tout}^{(L)}(10.2)$	x(3.8)	6.3	0.248 ± 0.005	0.332 ± 0.002	0.500 ± 0.012

Table 2a: Fit result for the independent jet model, 2^{nd} order QCD.

Distributions (χ^2/d.f.)			overall χ^2/d.f.	α_s	σ_q (GeV/c)	a_L
$Q_2(2.0)$	$Q_1(2.9)$	$x(4.8)$	3.9	0.158 ± 0.004	0.360 ± 0.004	0.661 ± 0.019
$L_2(1.4)$	$L_1(3.3)$	$x(5.5)$	4.2	0.147 ± 0.003	0.349 ± 0.004	0.648 ± 0.017
$p_{Tin}^{(Q)}(3.6)$	$p_{Tout}^{(Q)}(2.8)$	$x(6.1)$	4.8	0.150 ± 0.002	0.349 ± 0.002	0.595 ± 0.013
$p_{Tin}^{(L)}(4.0)$	$p_{Tout}^{(L)}(2.2)$	$x(6.8)$	5.0	0.156 ± 0.002	0.341 ± 0.002	0.551 ± 0.012

Table 2b: Fit results for the Lund string model, 2^{nd} order QCD.

Distributions (χ^2/d.f.)			overall χ^2/d.f.	α_s	σ_q (GeV/c)	a_L
$Q_2(1.3)$	$Q_1(3.0)$	$x(4.2)$	3.3	0.212 ± 0.003	0.317 ± 0.004	0.416 ± 0.018
$L_2(2.4)$	$L_1(11.9)$	$x(4.1)$	5.4	0.219 ± 0.003	0.309 ± 0.004	0.344 ± 0.016
$p_{Tin}^{(Q)}(2.2)$	$p_{Tout}^{(Q)}(5.3)$	$x(4.5)$	4.2	0.192 ± 0.003	0.327 ± 0.003	0.452 ± 0.014
$p_{Tin}^{(L)}(4.2)$	$p_{Tout}^{(L)}(7.8)$	$x(4.3)$	5.4	0.193 ± 0.003	0.320 ± 0.003	0.432 ± 0.013

Table 3: Values of α_s with χ^2/d.f. in brackets from fits to the perturbative regions. The independent jet model is used for fragmentation.

distribution	$O(\alpha_s)$	$O(\alpha_s^2)$		
ε	0.2	0.2	0.15	0.25
δ	40^o	40^o	34.5^o	45^o
σ_q	0.35 GeV/c	0.35 GeV/c	0.34 GeV/c	0.355 GeV/c
a_L	0.63	0.61	0.49	0.68
$Q_2 > 0.12$	0.215 ± 0.007 (9/5)	0.161 ± 0.004 (12/5)	0.155 ± 0.004 (7/5)	0.174 ± 0.004 (13/5)
$L_2 > 0.18$	0.208 ± 0.006 (1/5)	0.153 ± 0.004 (3/5)	0.148 ± 0.003 (3/5)	0.165 ± 0.004 (2/5)
$p_{TIN}^{(Q)} > 1$ GeV/c	0.187 ± 0.004 (55/10)	0.153 ± 0.003 (37/10)	0.145 ± 0.002 (38/10)	0.167 ± 0.003 (61/10)
$p_{TIN}^{(L)} > 1$ GeV/c	0.194 ± 0.004 (43/10)	0.157 ± 0.003 (40/10)	0.148 ± 0.002 (29/10)	0.173 ± 0.003 (48/10)
$\Delta M^2 > 0.08$	0.196 ± 0.010 (3/6)	0.155 ± 0.007 (2/6)	0.148 ± 0.006 (5/6)	0.175 ± 0.007 (4/6)

Table 4: Values of α_s with χ^2/d.f. in brackets from fits to the perturbative regions. The Lund string model is used for fragmentation

distribution \	$O(\alpha_s)$	$O(\alpha_s^2)$		
ε	0.2	0.2	0.15	0.25
δ	40	40	34.5	45
σ_q	0.33 GeV/c	0.32 GeV/c	0.31 GeV/c	0.335 GeV/c
a_L	0.47	0.41	0.43	0.45
$Q_2 > 0.12$	0.293 ± 0.008 (20/5)	0.208 ± 0.005 (12/5)	0.202 ± 0.004 (14/5)	0.215 ± 0.005 (13/5)
$L_2 > 0.18$	0.299 ± 0.007 (6/5)	0.213 ± 0.004 (2/5)	0.207 ± 0.004 (5/5)	0.217 ± 0.005 (1/5)
$p_{TIN}^{(Q)} > 1$ GeV/c	0.262 ± 0.005 (14/10)	0.194 ± 0.003 (7/10)	0.186 ± 0.003 (14/10)	0.209 ± 0.003 (6/10)
$p_{TIN}^{(L)} > 1$ GeV/c	0.256 ± 0.005 (32/10)	0.192 ± 0.003 (26/10)	0.181 ± 0.003 (30/10)	0.208 ± 0.003 (14/10)
$\Delta M^2 > 0.08$	0.313 ± 0.011 (5/6)	0.230 ± 0.008 (6/6)	0.217 ± 0.007 (6/6)	0.234 ± 0.009 (8/6)

Table 5a: Fit results for the independent jet model with $g \to q\bar{q}$, 2^{nd} order QCD.

Distributions (χ^2/d.f.)			overall χ^2/d.f.	α_s	σ_q (GeV/c)	a_L
$Q_2(2.8)$	$Q_1(6.8)$	x(6.6)	5.9	0.162 ± 0.004	0.377 ± 0.003	0.500 ± 0.023
$L_2(4.3)$	$L_1(3.3)$	x(6.9)	7.1	0.137 ± 0.003	0.367 ± 0.004	0.576 ± 0.019
$p_{Tin}^{(Q)}(2.8)$	$p_{Tout}^{(Q)}(3.0)$	x(9.7)	6.3	0.171 ± 0.003	0.353 ± 0.002	0.343 ± 0.013
$p_{Tin}^{(L)}(4.0)$	$p_{Tout}^{(L)}(2.5)$	x(10.8)	7.1	0.173 ± 0.003	0.346 ± 0.002	0.318 ± 0.012

Table 5b: Values of α_s in 2^{nd} order QCD (with χ^2/d.f. in brackets) from fits to the perturbative regions. The independent jet model with $g \to q\bar{q}$ is used. The parameters ε, δ, σ_q, a_L have been set to 0.20, 40^0, 0.36 GeV/c, 0.43.

Distributions		
$Q_2 > 0.12$	0.177 ± 0.004	(14/5)
$L_2 > 0.18$	0.165 ± 0.004	(3/5)
$p_{Tin}^{(Q)} > 1$ GeV/c	0.176 ± 0.003	(27/10)
$p_{Tin}^{(L)} > 1$ GeV/c	0.178 ± 0.003	(52/10)
$\Delta M^2 > 0.08$	0.170 ± 0.008	(4/6)

Table 6: Values for α_s in 2^{nd} order QCD from fits to a) the cluster-thrust (t_{CL}) distribution of 3-jet events and b) the 3-jet thrust (t_{GS}) distribution computed by the method of generalized sphericity. The χ^2/d.o.f. is given in brackets. The second column gives the fraction of all 16 219 events satisfying the t_{CL} or t_{GS} cuts indicated.

distribution		event fraction %	Independent jet model g = q, ε = 0.20, δ = 40°	Lund string model ε = 0.20, δ = 40°
a)	t_{CL} < 0.94	6.8	0.142 ± 0.004 (6.0/3)	0.183 ± 0.005 (4.8/3)
	< 0.90	4.0	0.137 ± 0.005 (2.8/2)	0.177 ± 0.006 (1.3/2)
	< 0.85	2.0	0.136 ± 0.005 (2.7/1)	0.174 ± 0.007 (0.8/1)
b)	t_{GS} < 0.94	10.7	0.147 ± 0.003 (10.1/5)	0.192 ± 0.004 (12.2/5)
	< 0.90	6.4	0.143 ± 0.004 (5.8/3)	0.188 ± 0.004 (5.9/3)
	< 0.85	3.3	0.141 ± 0.005 (5.5/2)	0.183 ± 0.006 (4.6/2)

Table 7: Values of α_s from fits to the asymmetry of the EWAC in the region $|\cos\chi| < 0.7$.

	model	ε	δ	α_s	$(\chi^2/\text{d.f.})$
a)	1^{st} order QCD:				
	indep. jet, g = q	0.20	40^o	0.166 ± 0.010	(16/5)
	string	0.20	40^o	0.253 ± 0.018	(12/5)
b)	2^{nd} order QCD, Extended FKSS :				
	indep. jet, g = q	0.20	40^o	0.139 ± 0.009	(12/5)
	string	0.20	40^o	0.190 ± 0.009	(9/5)
	indep. jet, g = q	0.15	34.5^o	0.142 ± 0.011	(16/5)
	indep. jet, g = q	0.25	45^o	0.142 ± 0.008	(12/5)
	indep. jet, g = $q\bar{q}$	0.20	40^o	0.157 ± 0.009	(17/5)
	indep. jet, g = q	0.20	40^o		
	no energy-momentum conservation			0.109 ± 0.007	(5/5)
c)	2^{nd} order QCD, ERT + AB :				
	indep. jet, g = q	0.20	40^o	0.117 $\pm$ 0.009	(9/5)
	indep. jet, g = $q\bar{q}$	0.20	40^o	0.127 $\pm$ 0.010	(12/5)
	string	0.20	40^o	0.159 $\pm$ 0.012	(10/5)

Figure Captions

Fig.1 1st order QCD fits.
The normalized distributions $1/\sigma_{tot}\ d\sigma/dX$ where X is the quantity indicated on the horizontal scale, for the corrected data (•) and for the best fit predictions of the independent jet model (——) and of the string model (---).

a,b) The scaled momentum distribution $x_p = 2p/W$. The histograms are from the fit to set Nr. 1 (see Sect. 5.3). The fits were performed in the region $0.02 < x_p < 0.7$. The data for $x_p < 0.01$ are not shown.

c,d) The eigenvalues Q_2 and Q_1 of the $T^{(2)}$ tensor. The histograms are from the fit to set. Nr. 1.

e,f) The eigenvalues L_2 and L_1 of the $T^{(1)}$ tensor. The histograms are from the fit to set Nr. 2.

g,h) The single particle inclusive $p_{T\ in}^{(Q)}$ and $p_{T\ out}^{(Q)}$ distributions. The momentum components refer to the eigenvectors of the $T^{(2)}$ tensor. The histograms are from the fit to set Nr. 3.

i,j) The single particle inclusive $p_{T\ in}^{(L)}$ and $p_{T\ out}^{(L)}$ distributions. The momentum components refer to the eigenvectors of the $T^{(1)}$ tensor. The histograms are from the fit to set Nr. 4.

k) The difference ΔM^2 between the higher and lower scaled jet mass squared. The histograms are from the perturbative fits (lowest row in Tables 3, 4).

Fig.2 Same as Fig. 1 for 2nd order QCD fits using Extended FKSS.

Fig.3 The normalized distribution $1/\sigma_{tot}\ d\sigma/dt_{CL}$ of 3-cluster thrust of the uncorrected data (•) and the predictions of the independent jet model (——) and of the string model (---) in 2nd order QCD (Extended FKSS) as obtained from fits to the region $t_{CL} < 0.94$.

Fig.4 The normalized distribution $1/\sigma_{tot}\ d\sigma/dt_{GS}$ of the 3-jet thrust computed with the method of generalized sphericity. Shown are the uncorrected data (•) and the predictions of the independent

jet model (——) and of the string model (---) in 2nd order QCD (Extended FKSS) as obtained from fits to the region $t_{GS} < 0.94$.

Fig.5 The asymmetric part of the energy-energy correlation function of the corrected data (ϕ) and the predictions of the independent jet model (——) and the string model (---) as obtained from fits to the region $|\cos\chi| < 0.7$.

a) 1st order QCD fits.

b) 2nd order QCD fits (Extended FKSS).

c) 2nd order QCD fits (ERT + AB).

Fig.6 Average of several jet measures as a function of the c.m. energy W. The corrected data (ϕ) are from this experiment as given in Ref. 42. The predictions of the 2nd order QCD independent jet model (——) and the string model (---) are drawn as curves.

a) average of sphericity S.

b) average of 1-thrust.

c) average of $\langle p_{T\ in}^2 \rangle$ and $\langle p_{T\ out}^2 \rangle$ of charged particles.

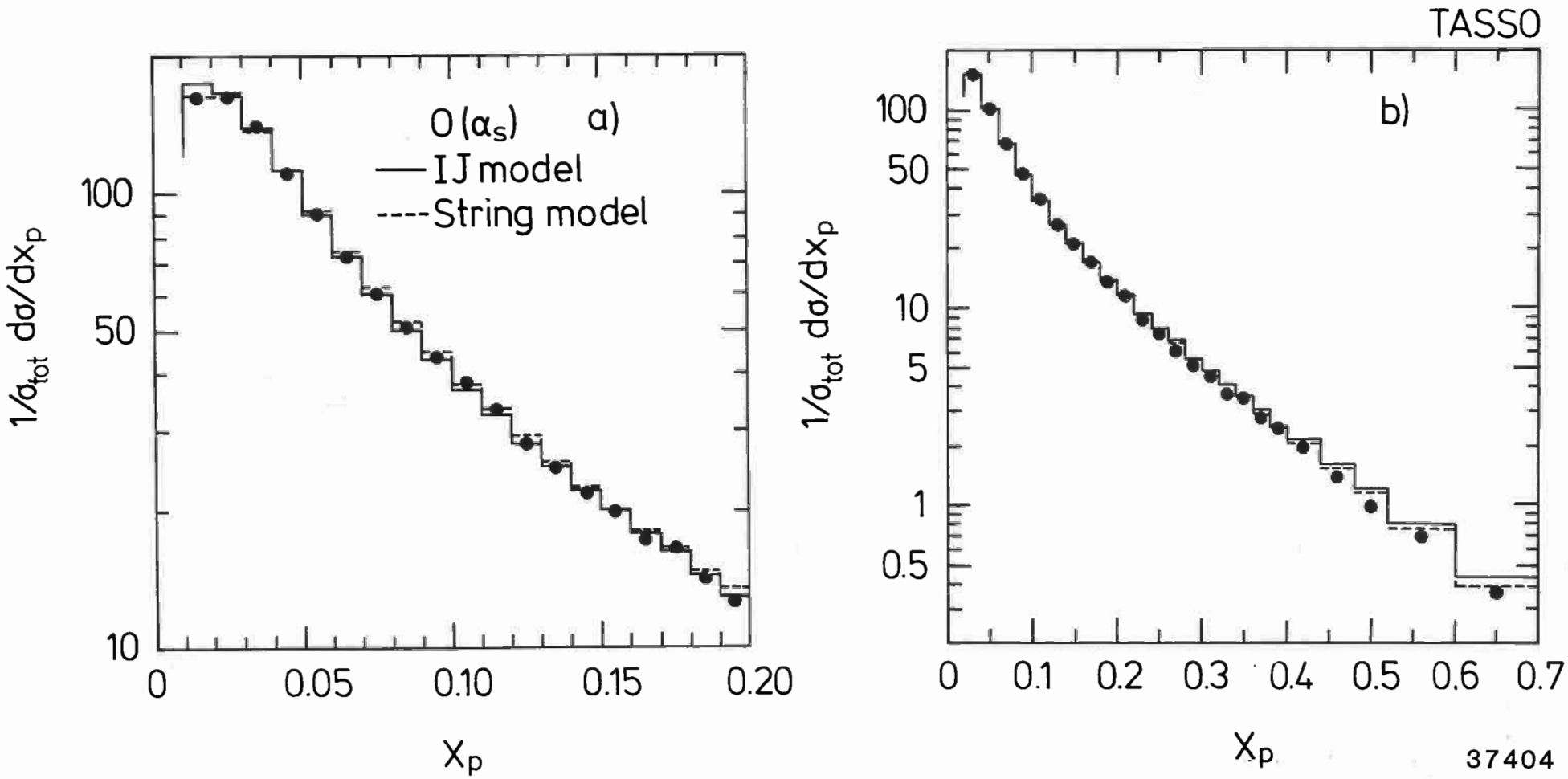
TASSO
O(αs) a)
IJ model
String model
100
50
10
1/σtot dσ/dxp
0
0.05
0.10
0.15
0.20
xp
b)
100
50
10
5
1
0.5
0
0.1
0.2
0.3
0.4
0.5
0.6
0.7
xp
37404

Fig. 1

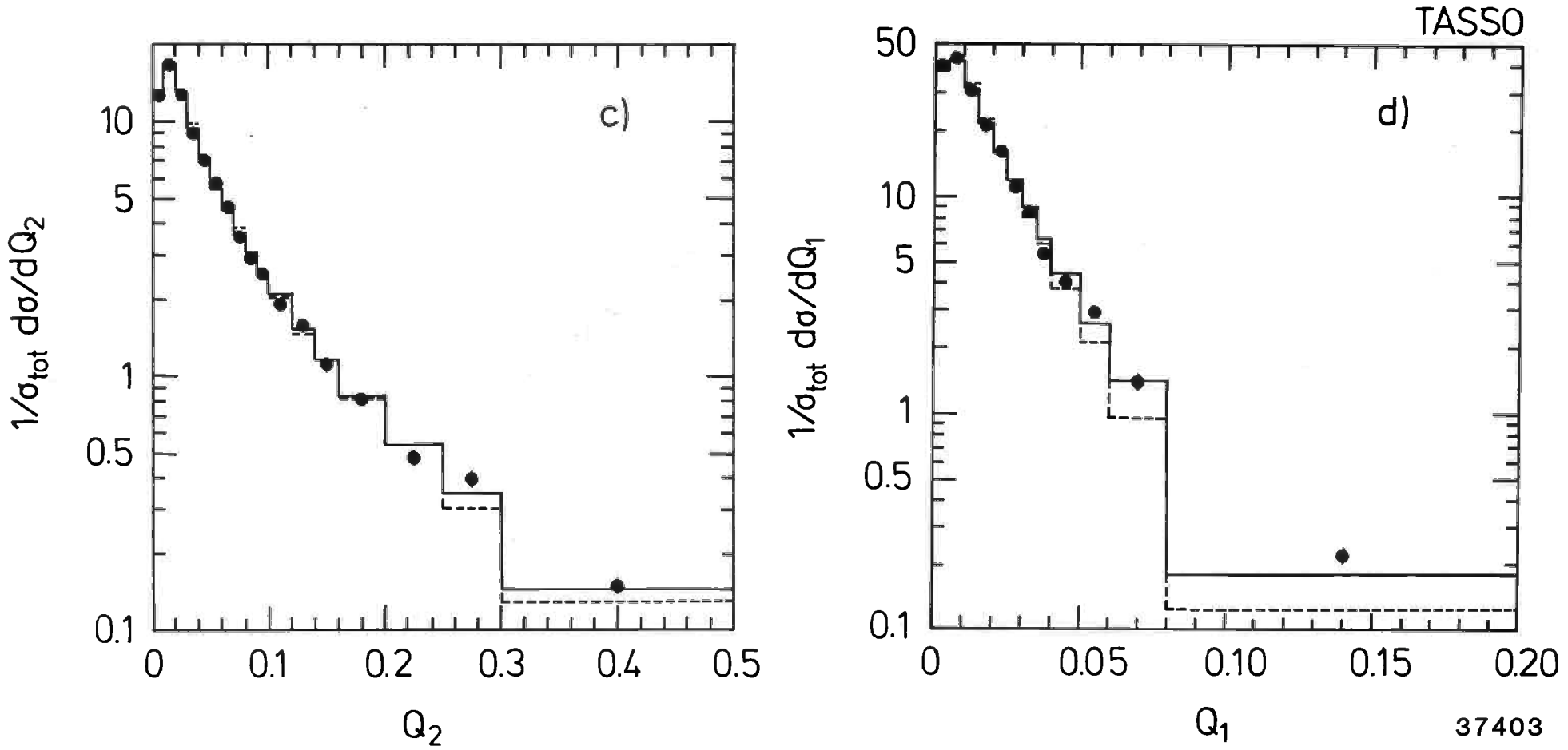
c)
d)
TASSO
$1/\sigma_{tot}\ d\sigma/dQ_2$
$1/\sigma_{tot}\ d\sigma/dQ_1$
Q_2
Q_1
10
5
1
0.5
0.1
50
0
0.1
0.2
0.3
0.4
0.5
0.05
0.10
0.15
0.20
37403

Fig. 1

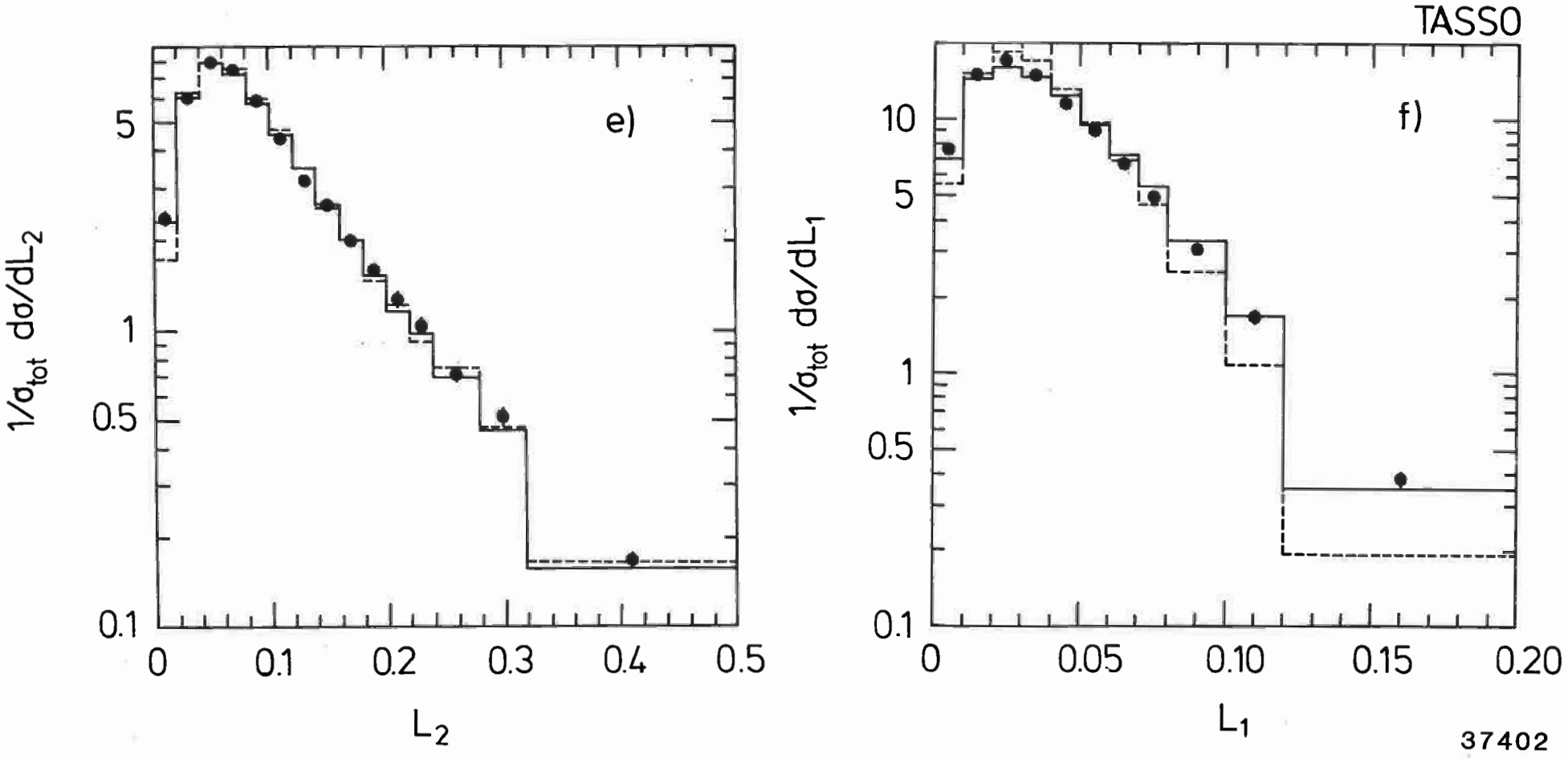
TASSO
e)
f)
$1/\sigma_{tot}\ d\sigma/dL_2$
$1/\sigma_{tot}\ d\sigma/dL_1$
L_2
L_1
0.1
0.5
1
5
10
0
0.1
0.2
0.3
0.4
0.5
0.05
0.10
0.15
0.20
37402

Fig. 1

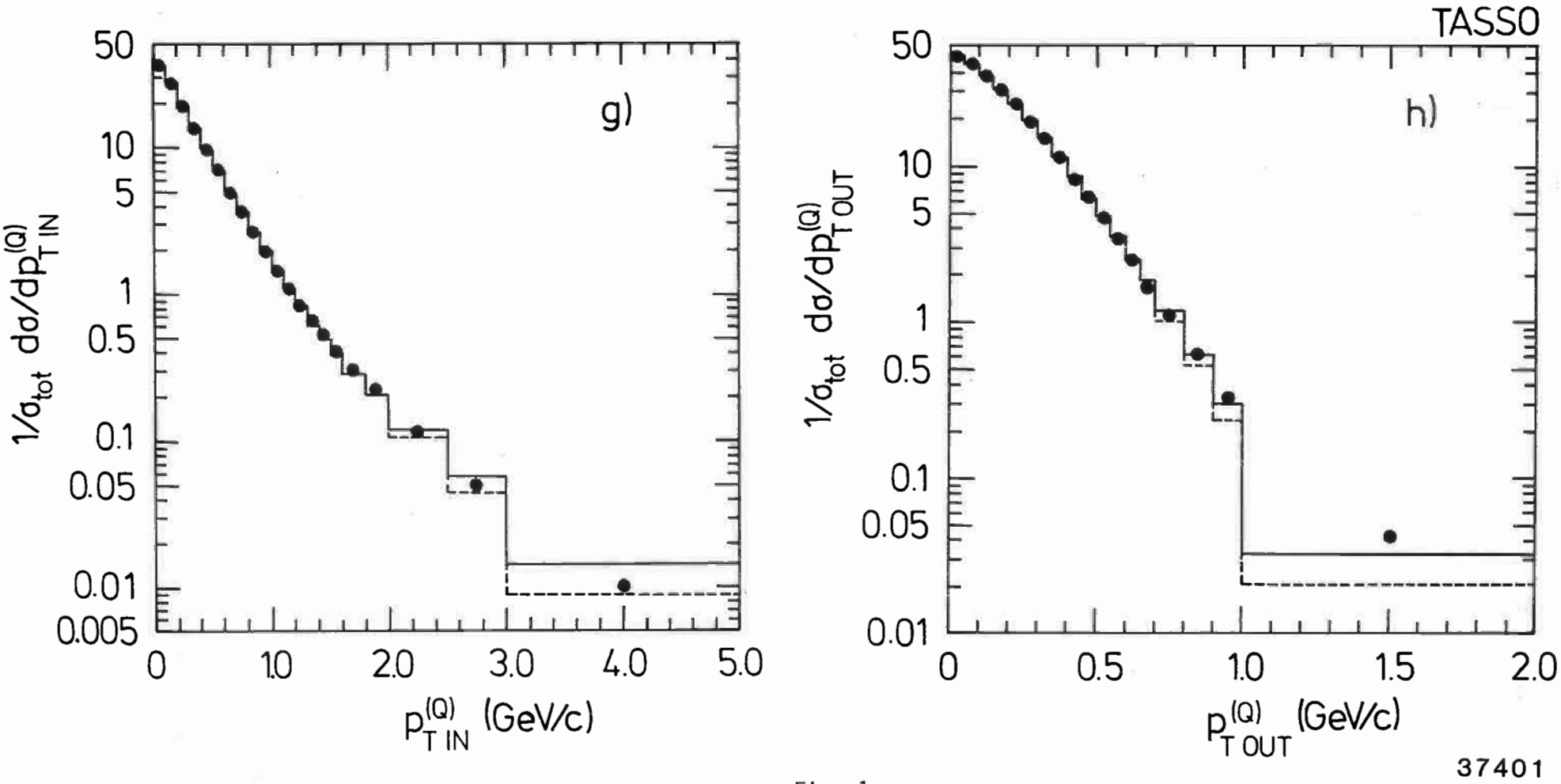
TASSO
g)
h)
50
10
5
1
0.5
0.1
0.05
0.01
0.005
0
1.0
2.0
3.0
4.0
5.0
0.5
1.5
$1/\sigma_{tot}\ d\sigma/dp_{T\,IN}^{(Q)}$
$1/\sigma_{tot}\ d\sigma/dp_{T\,OUT}^{(Q)}$
$p_{T\,IN}^{(Q)}$ (GeV/c)
$p_{T\,OUT}^{(Q)}$ (GeV/c)
37401

Fig. 1

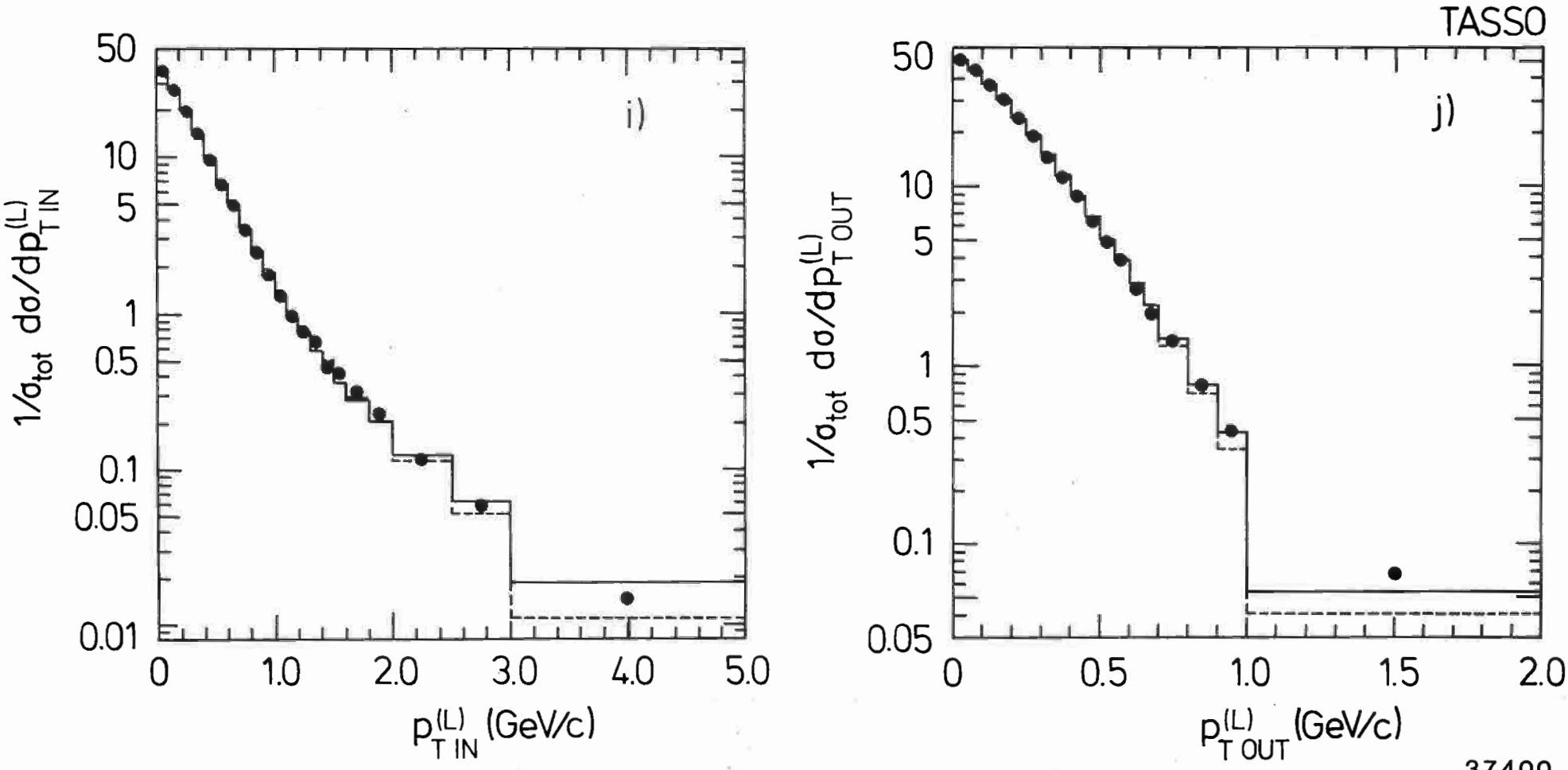
TASSO
i)
j)
$1/\sigma_{tot}\ d\sigma/dp_{T\,IN}^{(L)}$
$1/\sigma_{tot}\ d\sigma/dp_{T\,OUT}^{(L)}$
$p_{T\,IN}^{(L)}$ (GeV/c)
$p_{T\,OUT}^{(L)}$ (GeV/c)
50
10
5
1
0.5
0.1
0.05
0.01
0
1.0
2.0
3.0
4.0
5.0
0.5
1.5
37400

Fig. 1

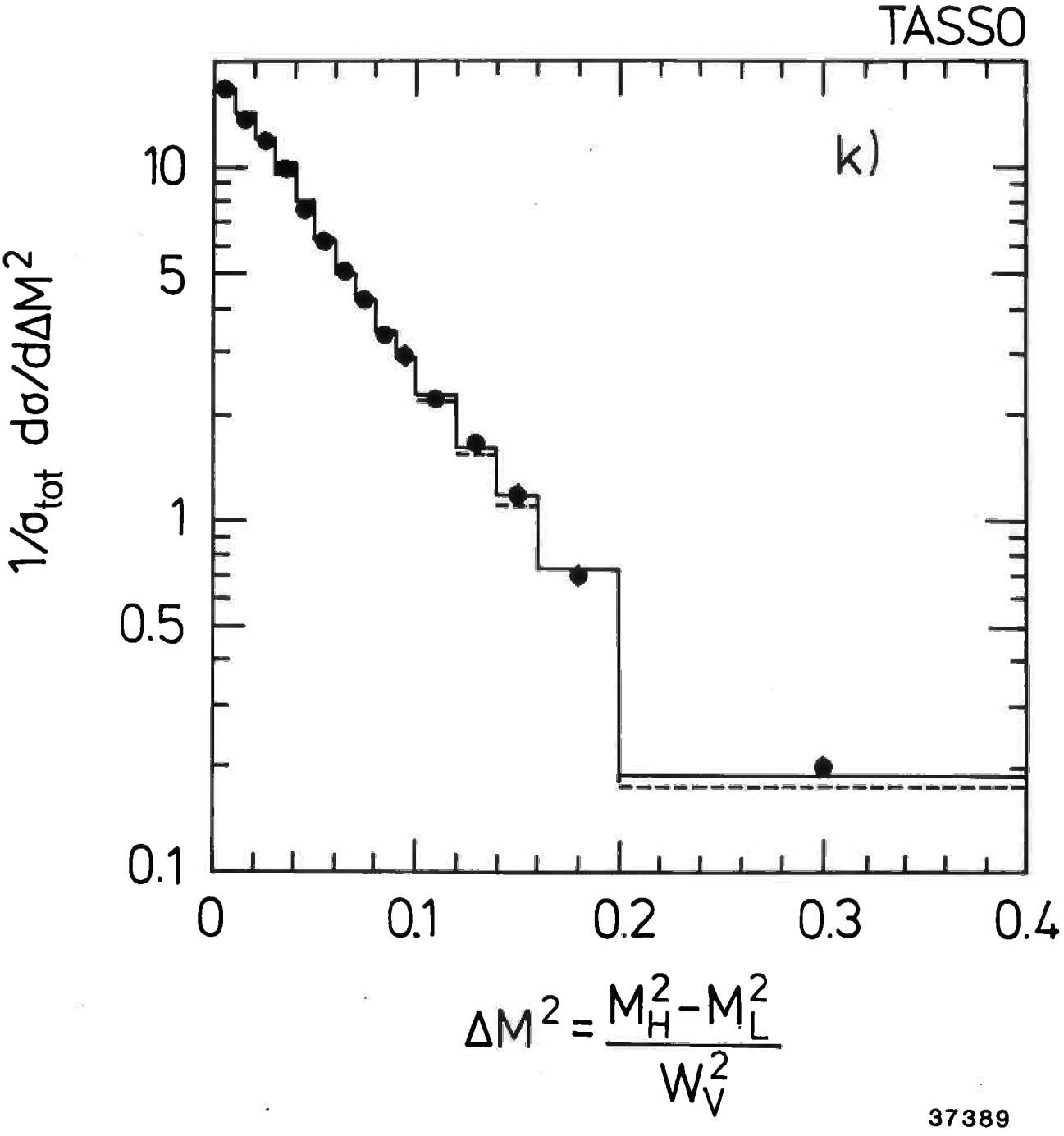
TASSO
k)
10
5
1
0.5
0.1
0
0.1
0.2
0.3
0.4
$1/\sigma_{tot}\ d\sigma/d\Delta M^2$
$\Delta M^2 = \frac{M_H^2 - M_L^2}{W_V^2}$
37389

Fig. 1

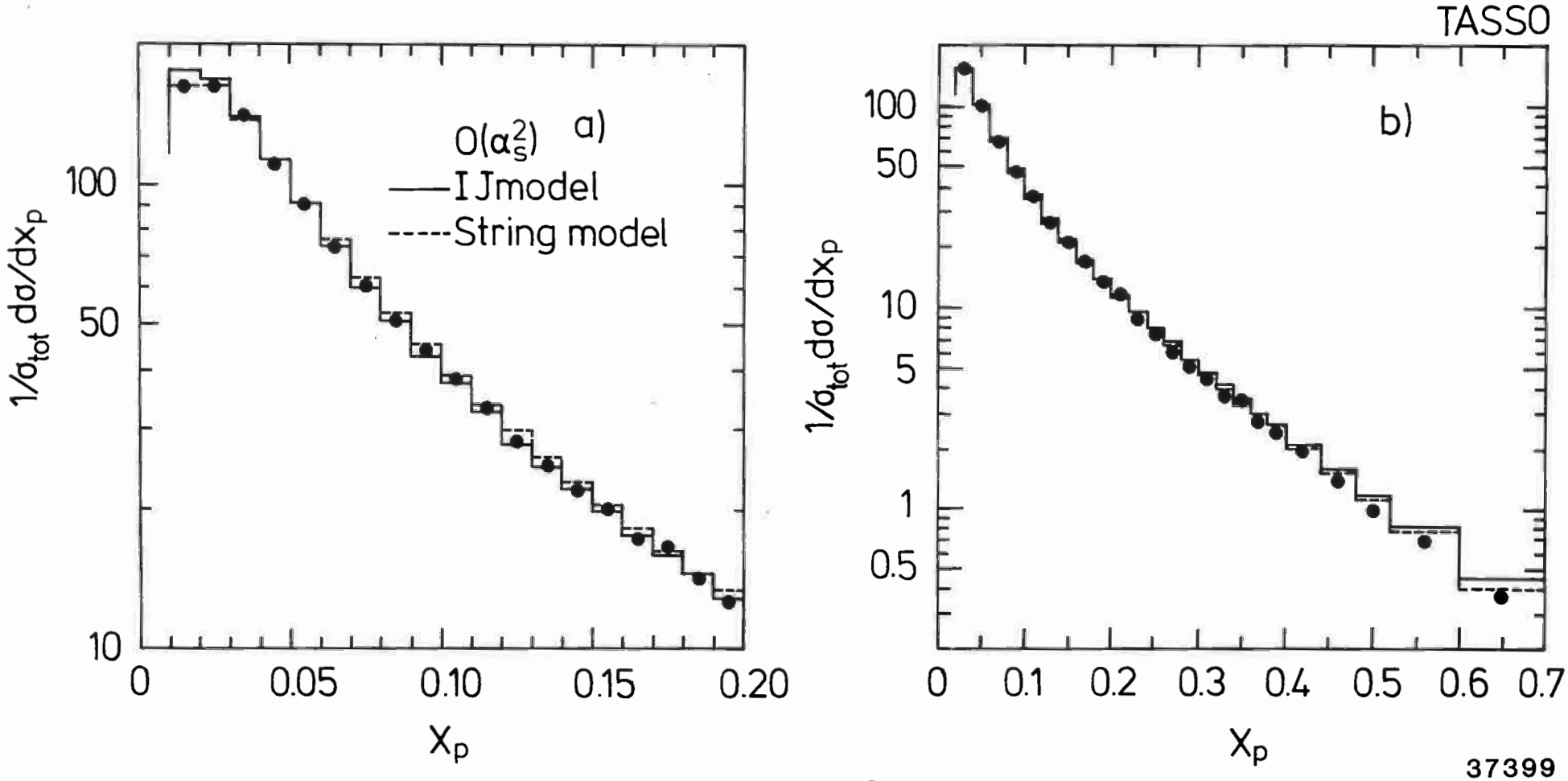
TASSO
a)
$O(\alpha_s^2)$
——IJmodel
-----String model
$1/\sigma_{tot}\, d\sigma/dx_p$
100
50
10
0
0.05
0.10
0.15
0.20
X_p
b)
100
50
10
5
1
0.5
0
0.1
0.2
0.3
0.4
0.5
0.6
0.7
X_p
37399

Fig. 2

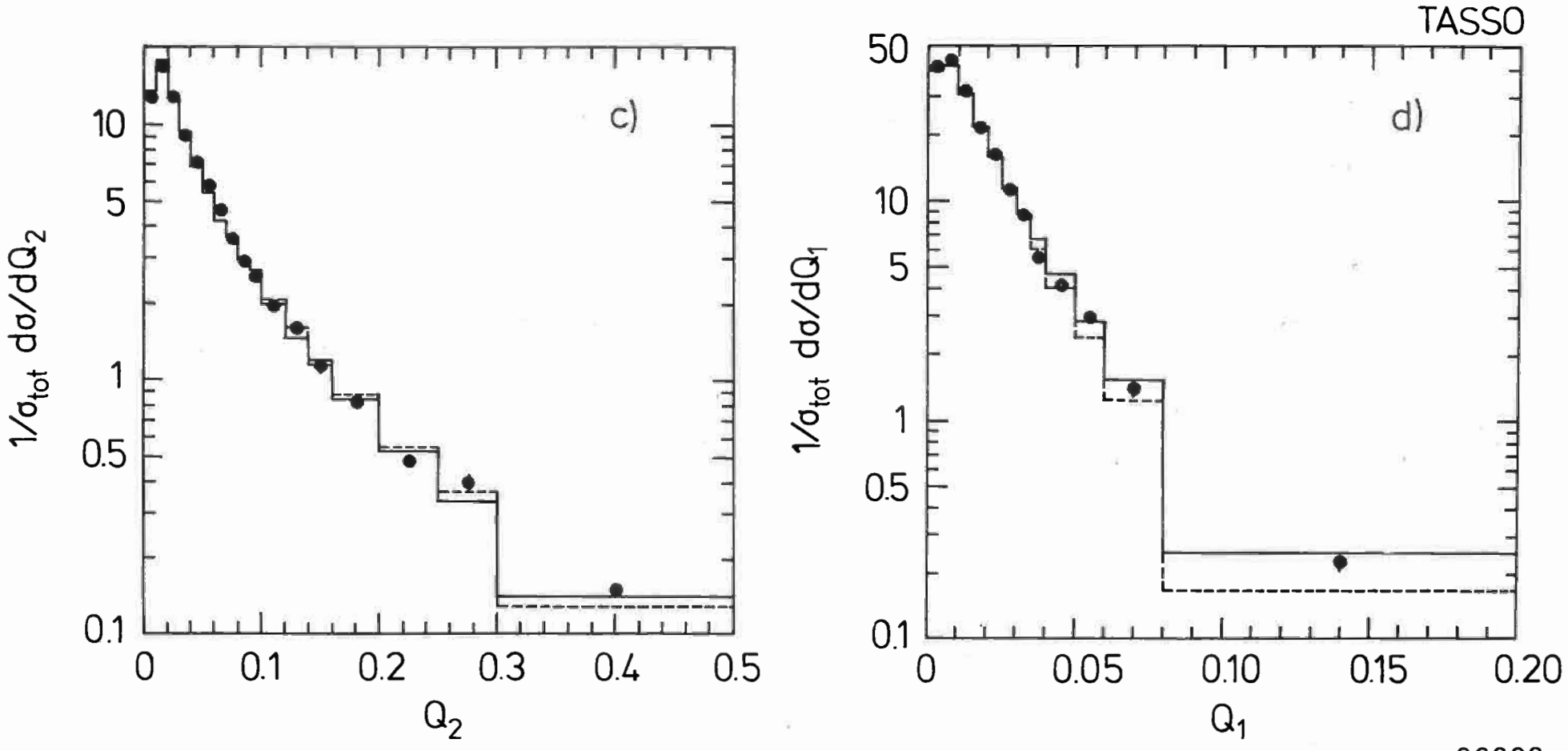
TASSO
c)
d)
$1/\sigma_{tot}\ d\sigma/dQ_2$
$1/\sigma_{tot}\ d\sigma/dQ_1$
Q_2
Q_1
10
5
1
0.5
0.1
50
0
0.1
0.2
0.3
0.4
0.5
0.05
0.10
0.15
0.20
36398

Fig. 2

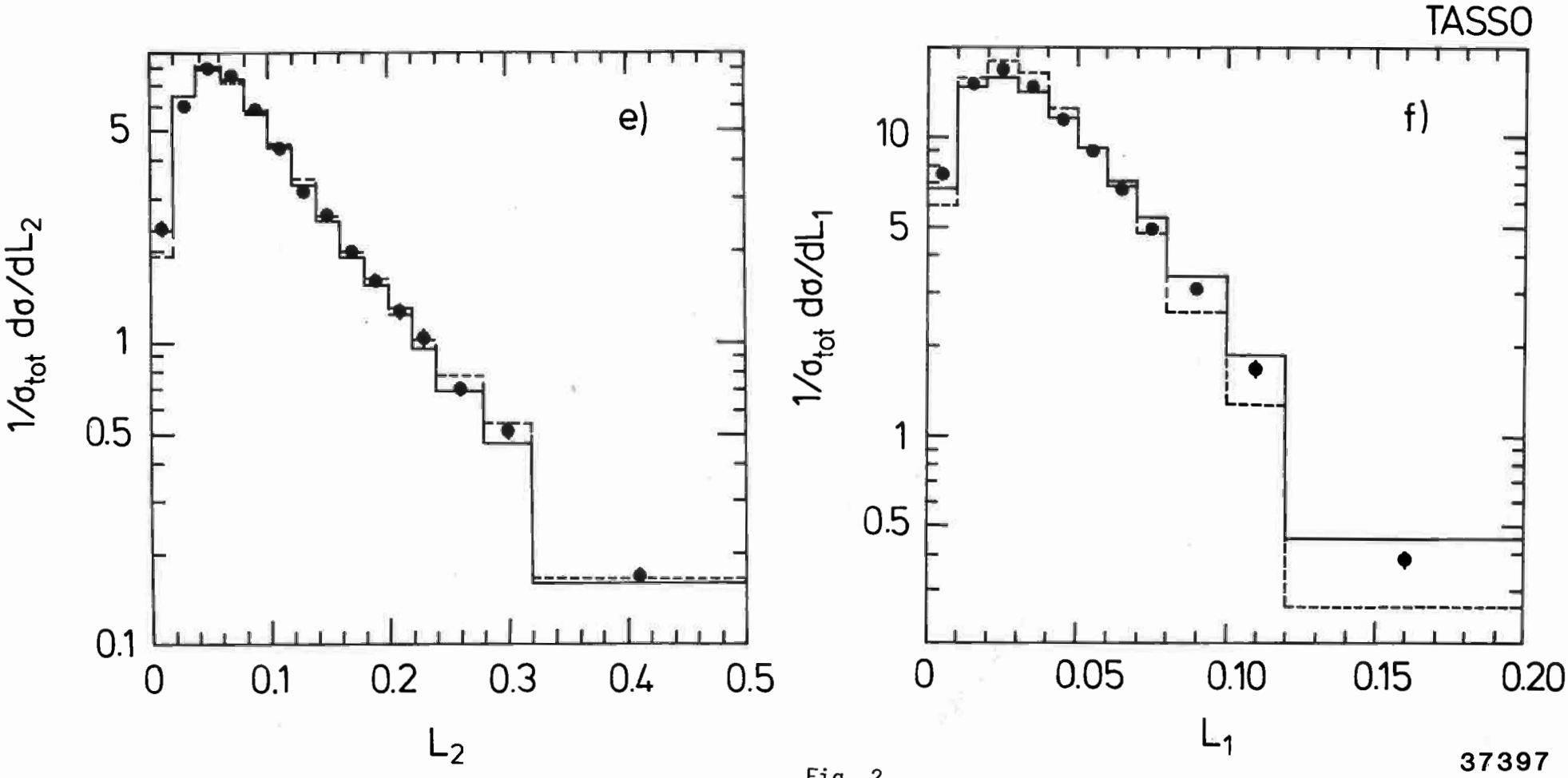
TASSO
e)
f)
$1/\sigma_{tot}\ d\sigma/dL_2$
$1/\sigma_{tot}\ d\sigma/dL_1$
L_2
L_1
0.1
0.5
1
5
10
0
0.1
0.2
0.3
0.4
0.5
0.05
0.10
0.15
0.20
37397

Fig. 2

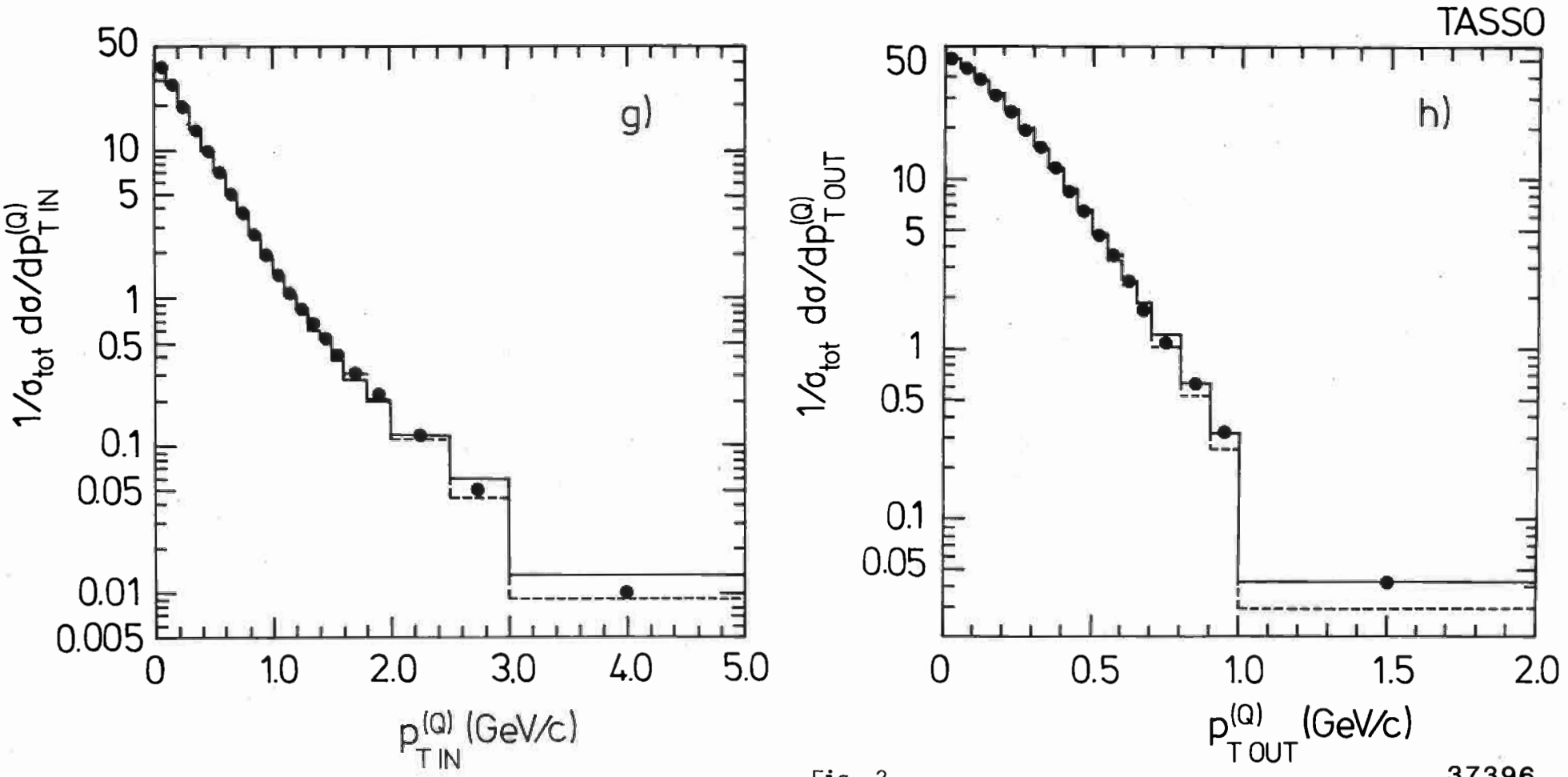
TASSO
g)
h)
$1/\sigma_{tot}\ d\sigma/dp_{T\,IN}^{(Q)}$
$1/\sigma_{tot}\ d\sigma/dp_{T\,OUT}^{(Q)}$
$p_{T\,IN}^{(Q)}$ (GeV/c)
$p_{T\,OUT}^{(Q)}$ (GeV/c)
50
10
5
1
0.5
0.1
0.05
0.01
0.005
0
1.0
2.0
3.0
4.0
5.0
0.5
1.5
37396

Fig. 2

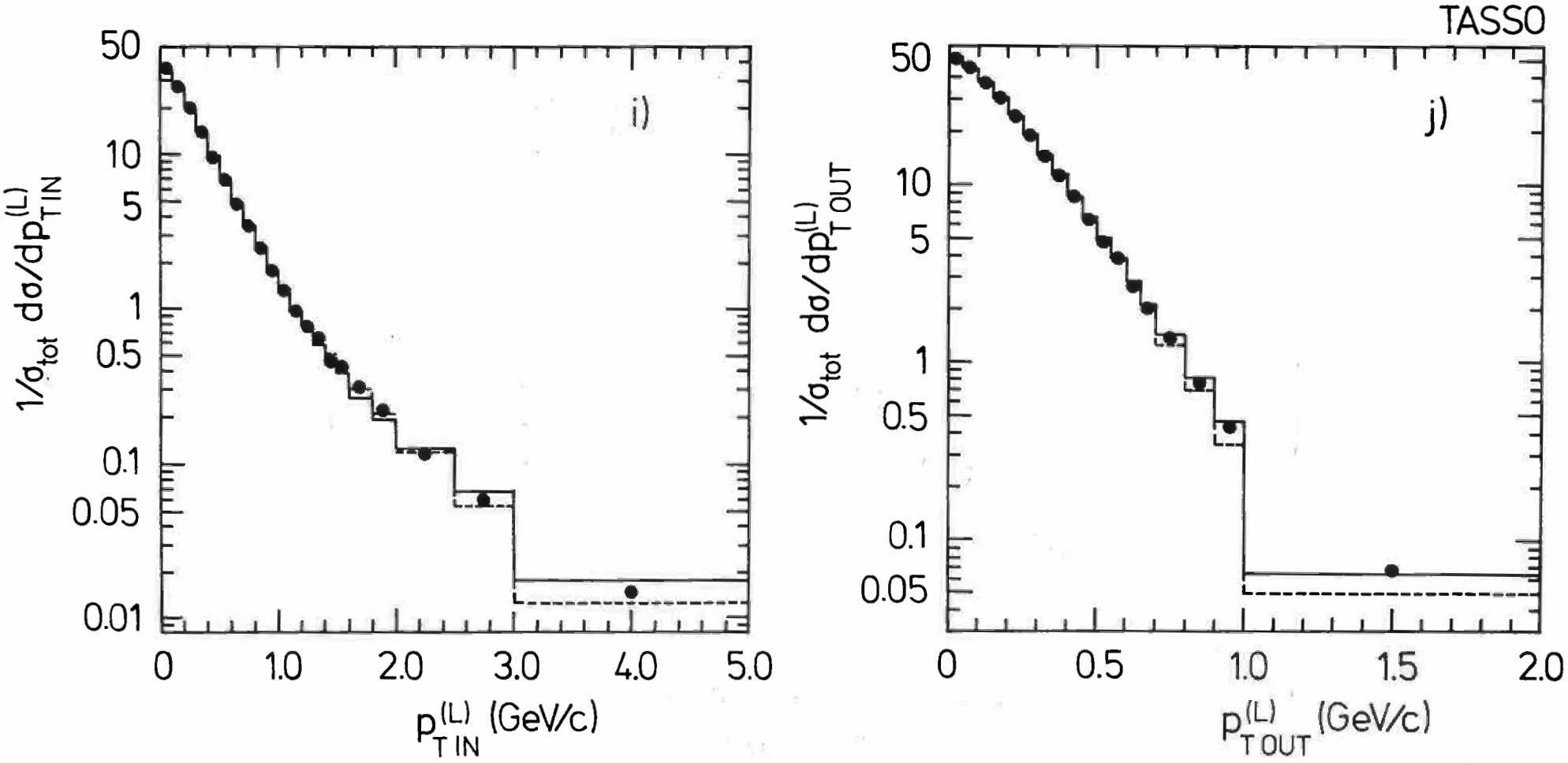
TASSO
i)
j)
50
10
5
1
0.5
0.1
0.05
0.01
0
1.0
2.0
3.0
4.0
5.0
0.5
1.5
$1/\sigma_{tot}\ d\sigma/dp_{T\,IN}^{(L)}$
$1/\sigma_{tot}\ d\sigma/dp_{T\,OUT}^{(L)}$
$p_{T\,IN}^{(L)}$ (GeV/c)
$p_{T\,OUT}^{(L)}$ (GeV/c)
37395

Fig. 2

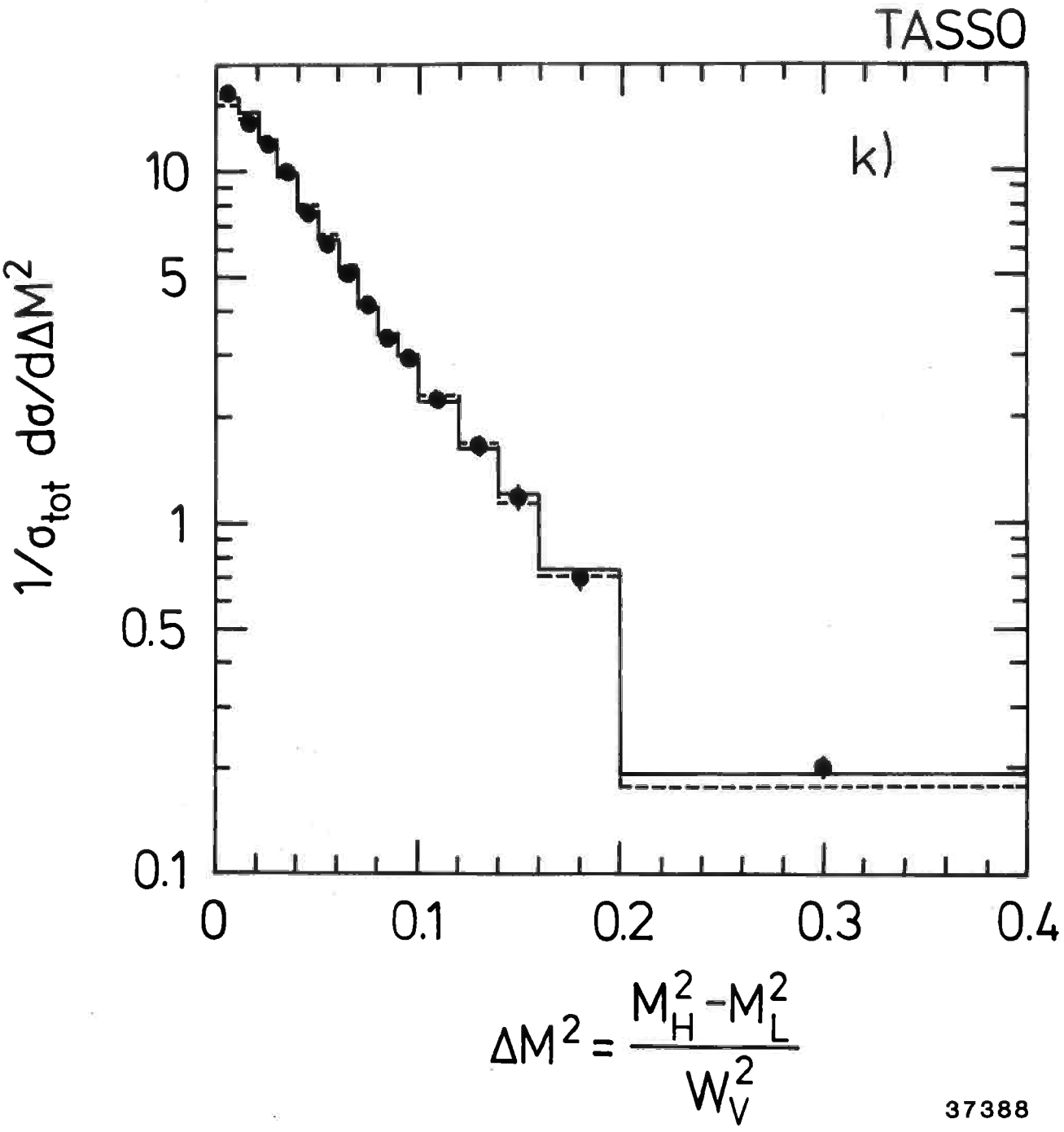
TASSO
k)
10
5
1
0.5
0.1
0
0.1
0.2
0.3
0.4
$1/\sigma_{tot}\ d\sigma/d\Delta M^2$
$\Delta M^2 = \frac{M_H^2 - M_L^2}{W_V^2}$
37388

Fig. 2

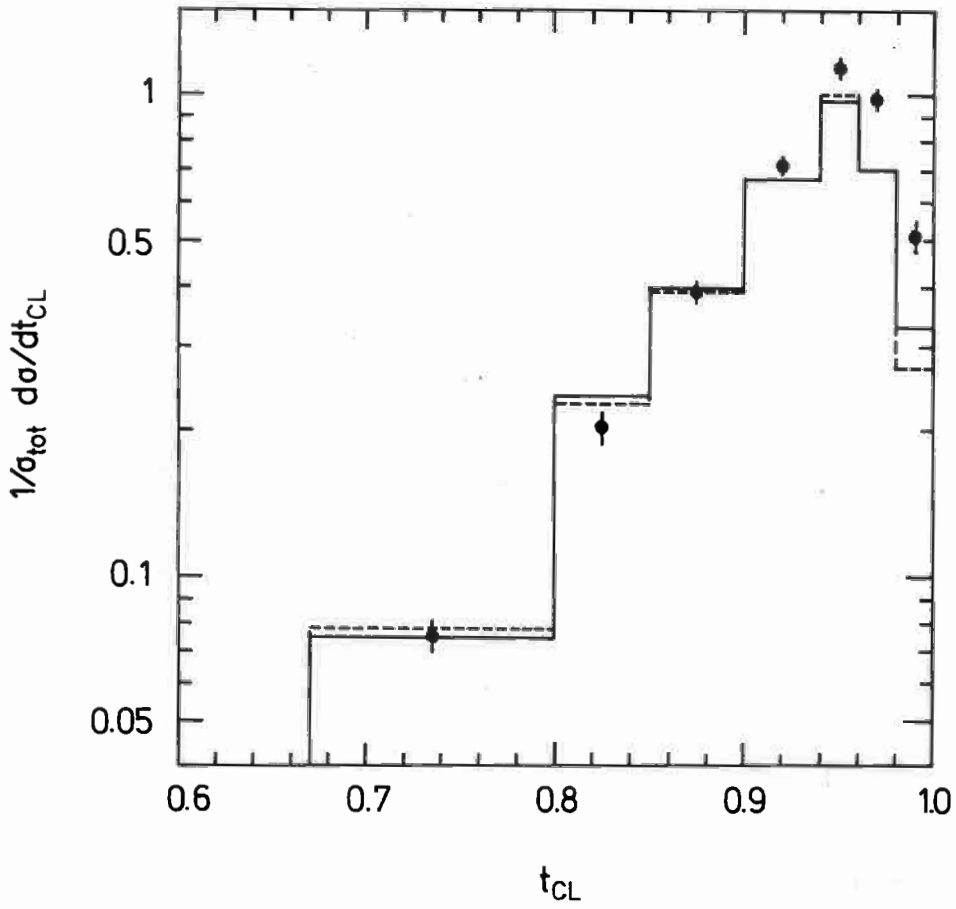
1
0.5
0.1
0.05
0.6
0.7
0.8
0.9
1.0
$1/\sigma_{tot}\ d\sigma/dt_{CL}$
t_{CL}

Fig. 3

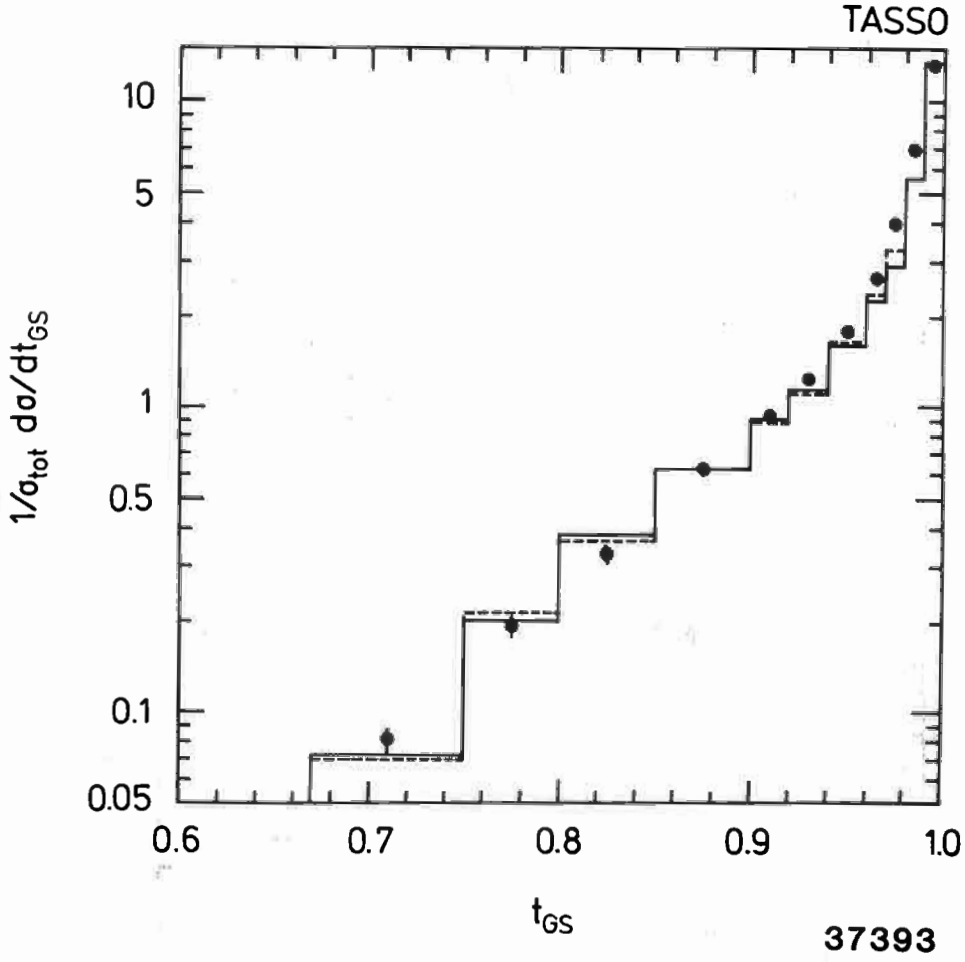
TASSO
10
5
1
0.5
0.1
0.05
0.6
0.7
0.8
0.9
1.0
$1/\sigma_{tot}\ d\sigma/dt_{GS}$
t_{GS}
37393

Fig. 4

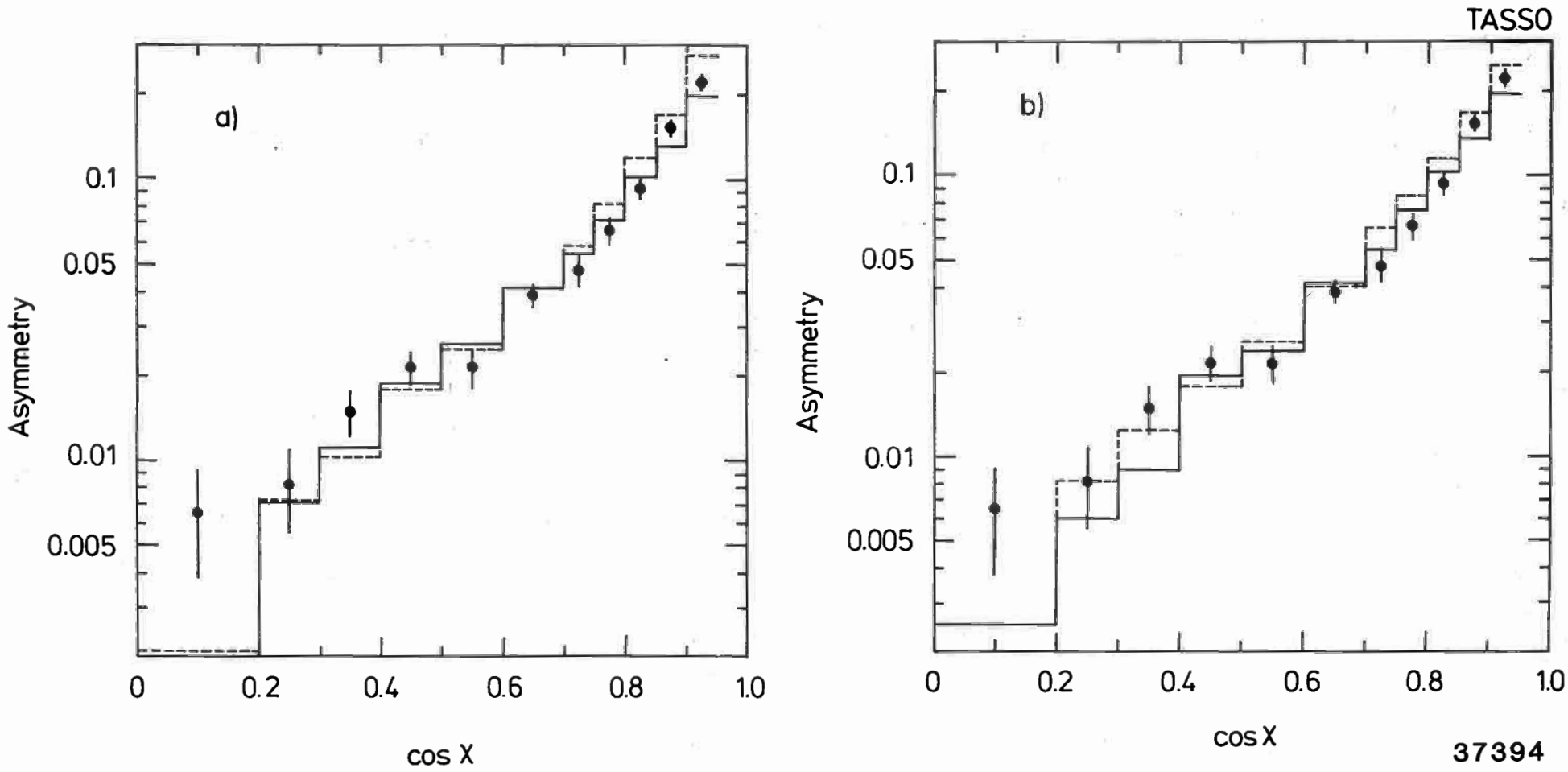

Fig. 5

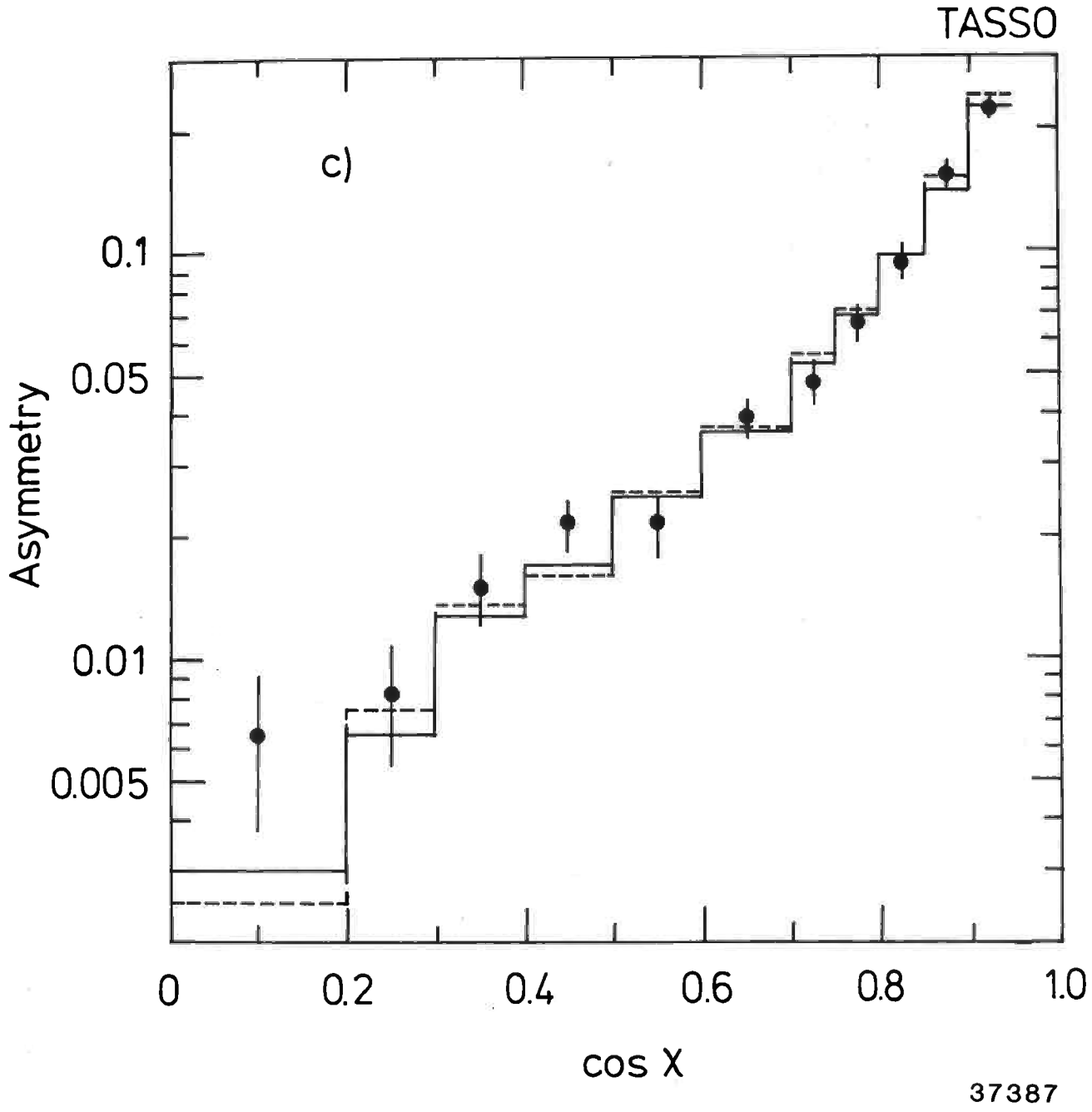

Fig. 5

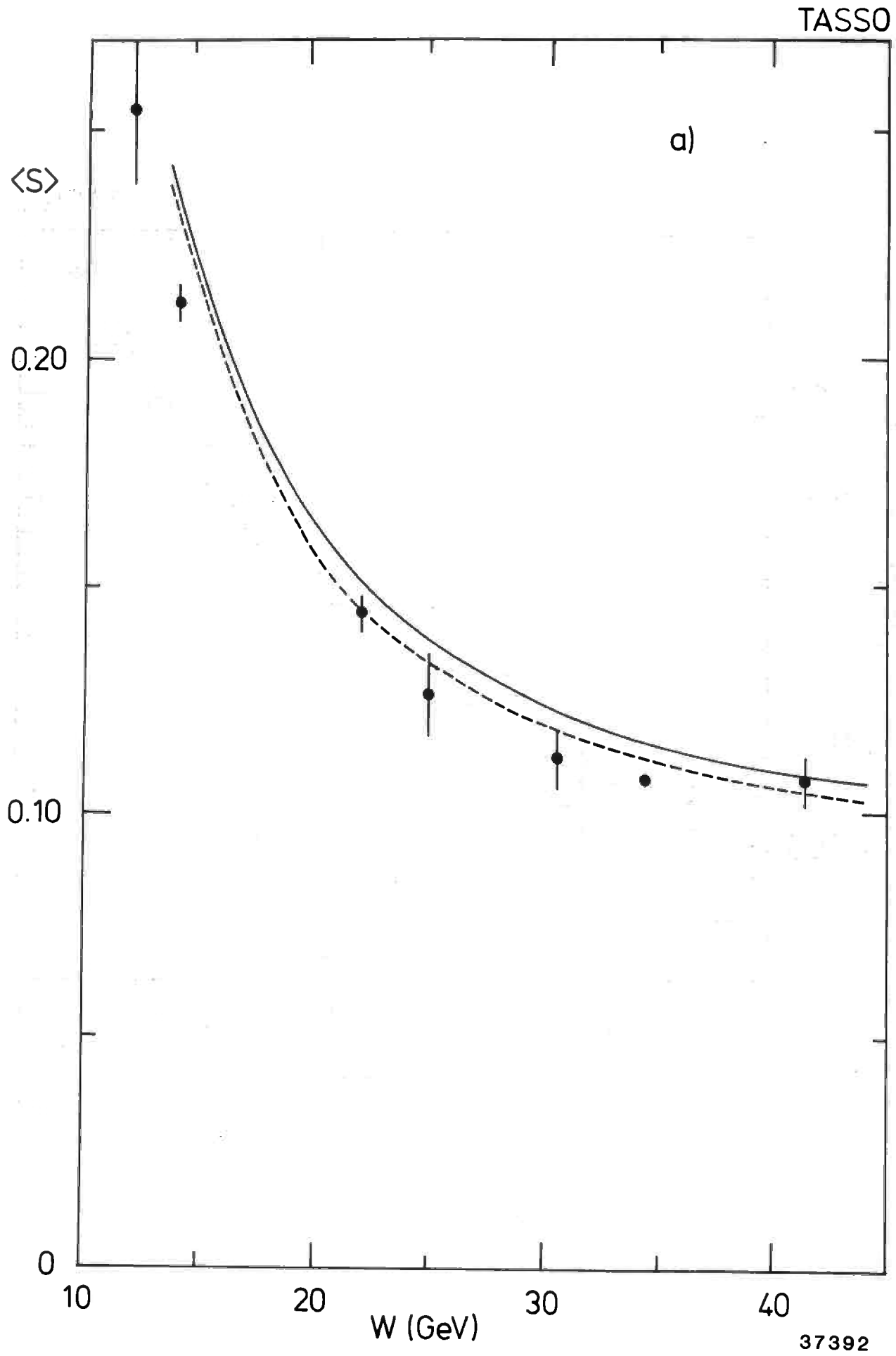

Fig. 6

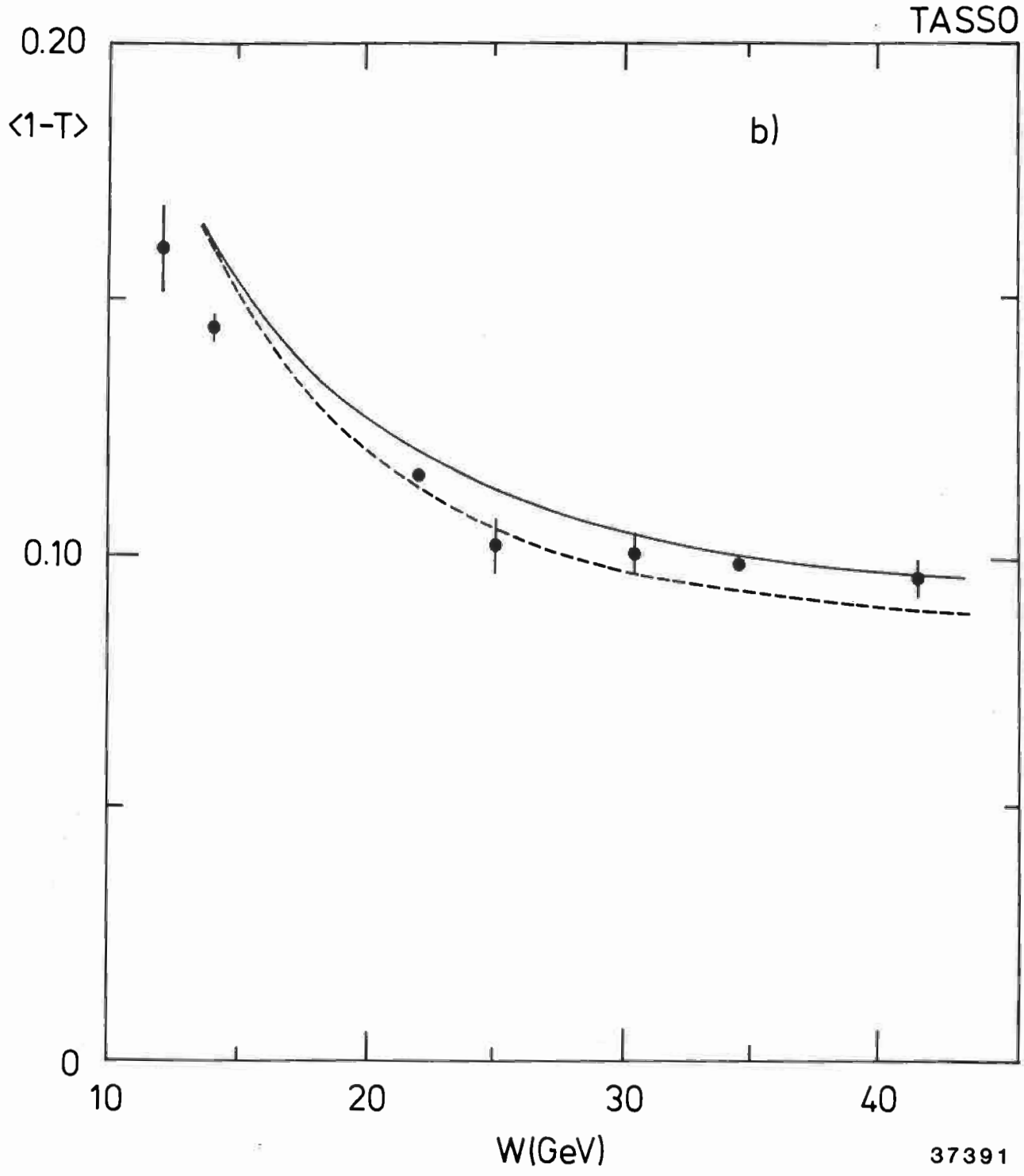

Fig. 6

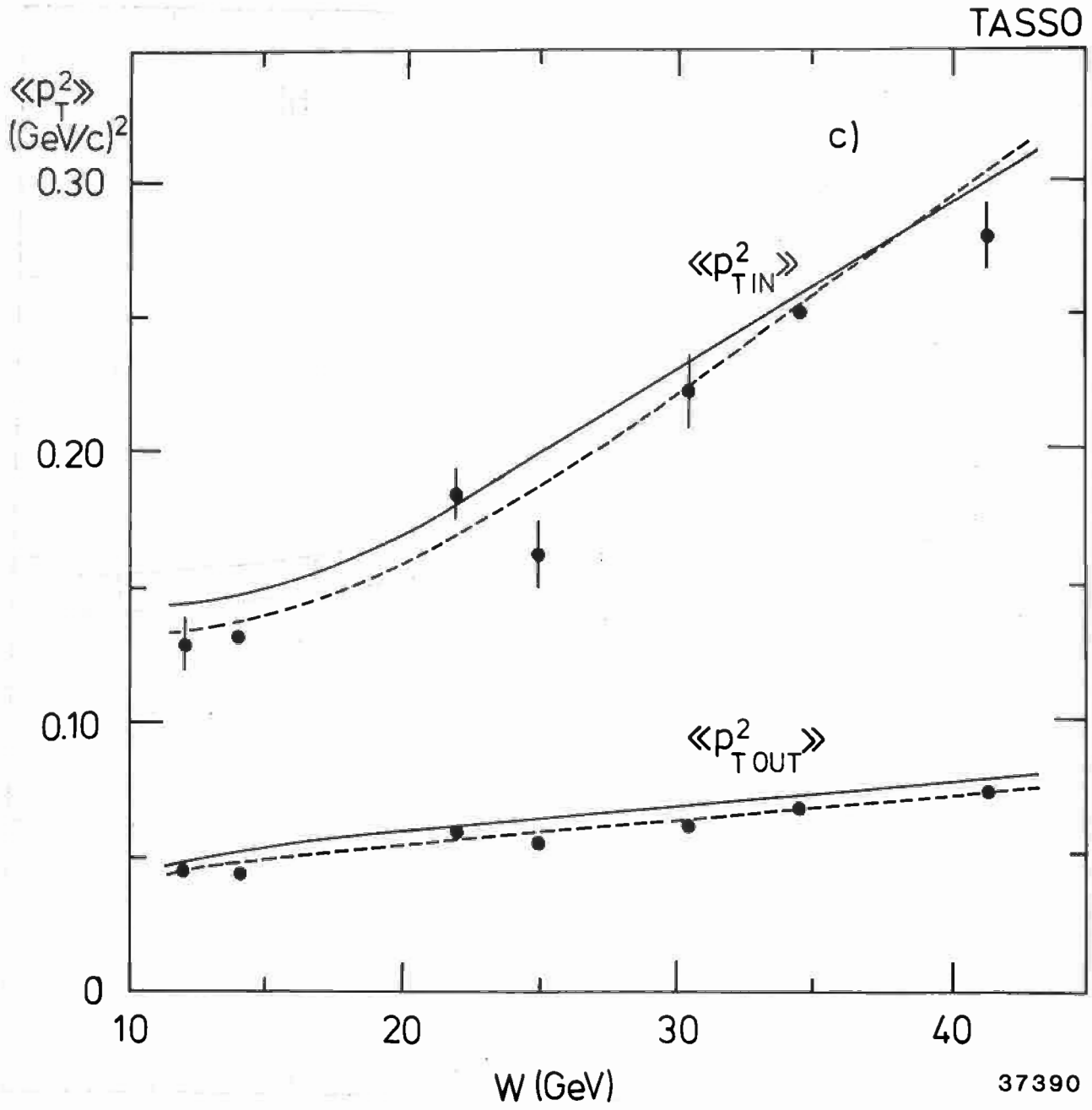
TASSO
«p²T»
(GeV/c)²
c)
0.30
0.20
0.10
0
«p²T IN»
«p²T OUT»
10
20
30
40
W (GeV)
37390

Fig. 6